

Impostor Among ν s: Dark Radiation Masquerading as Self-Interacting Neutrinos

Anirban Das ^{1,2,*}, P. S. Bhupal Dev ^{3,4,†}, Christina Gao ^{5,‡}, Subhajit Ghosh ^{6,§} and Taegyun Kim ^{7,5,¶}

¹*Theory Division, Saha Institute of Nuclear Physics, 1/AF, Bidhannagar, Kolkata 700064, India*

²*Homi Bhabha National Institute, Training School Complex, Anushaktinagar, Mumbai 400094, India*

³*Department of Physics and McDonnell Center for the Space Sciences,
Washington University, St. Louis, MO 63130, USA*

⁴*PRISMA⁺ Cluster of Excellence & Mainz Institute for Theoretical Physics,
Johannes Gutenberg-Universität Mainz, 55099 Mainz, Germany*

⁵*Department of Physics, Southern University of Science and Technology, Shenzhen, 518055, China*

⁶*Texas Center for Cosmology and Astroparticle Physics, Weinberg Institute,*

Department of Physics, The University of Texas at Austin, Austin, TX 78712, USA

⁷*Uichang District Office, 468, Dogye-dong, Uichang-gu, Changwon, 51381, South Korea*

Multiple cosmological observations hint at neutrino self-interactions beyond the Standard Model, yet such interactions face severe constraints from terrestrial experiments. We resolve this tension by introducing a model where active neutrinos resonantly convert to self-interacting dark radiation after BBN but before CMB epoch. This exploits the fact that cosmological observables cannot distinguish between neutrinos and dark radiation with the same abundance and free-streaming properties. Our mechanism, based on a simple Type-I seesaw framework along with a keV-scale scalar mediator, achieves two objectives: (1) it produces strongly self-interacting dark radiation that imitates neutrino self-interactions favored by cosmological data, and (2) it depletes the active neutrino energy density, relaxing cosmological neutrino mass bounds and easing the tension with neutrino oscillation data. The model naturally evades laboratory constraints through suppression of the neutrino-mediator coupling by the squared mass ratio of active and sterile neutrinos. We demonstrate how this scenario is favored over Λ CDM by the combined Planck and DESI data, while being consistent with all other constraints. Our mechanism is testable in future laboratory probes of absolute neutrino mass and searches for sterile neutrinos.

INTRODUCTION

Neutrinos, as the most elusive Standard Model (SM) particles, may hold the key to discovering new physics. While the SM predicts neutrinos to be massless, neutrino oscillation experiments have precisely measured two non-zero mass-squared differences, namely, $\Delta m_{\text{sol}}^2 \simeq 7.5 \times 10^{-5} \text{ eV}^2$ and $\Delta m_{\text{atm}}^2 \simeq 2.5 \times 10^{-3} \text{ eV}^2$ [1], indicating that at least two of the three neutrino mass eigenvalues must be non-zero. Despite this breakthrough, the absolute neutrino mass scale, i.e., whether the lightest neutrino has non-zero mass, remains unknown. A direct and model-independent laboratory constraint on the absolute neutrino mass comes from the kinematics of beta decay or electron capture. Currently, KATRIN has the best direct limit on $m_\nu < 0.45 \text{ eV}$ at 90% confidence level [2], with a design sensitivity of 0.2 eV [3], while the proposed Project 8 experiment aims for 0.04 eV [4].

Precision cosmology provides an alternative indirect way to measure the *total* neutrino mass. In the standard cosmological model, neutrinos decouple from the thermal bath during Big Bang Nucleosynthesis (BBN) at a temperature around 1 MeV. Afterward, neutrinos continue to free-stream until their temperature falls below their mass, making them non-relativistic. Relativistic neutrinos suppress the growth of structure because they do not cluster and hinder the clustering of other matter through radiation pressure [5]. This characteristic suppression of the matter power spectrum makes cosmological probes

such as the Cosmic Microwave Background (CMB) and the Baryon Acoustic Oscillations (BAO) sensitive to neutrino mass. The strongest constraint to date on the total neutrino mass, $\sum m_\nu < 0.0642 \text{ eV}$ at 95% CL, comes from Planck + DESI-II BAO analysis [6, 7], surpassing current laboratory constraints by an order of magnitude.

Cosmological measurements of neutrino mass are growingly in tension with neutrino oscillation experiments, which require $\sum m_\nu > 0.059$ (0.10) eV for the normal (inverted) mass ordering [1]. Thus, current cosmological constraints strongly disfavor the inverted ordering, and the parameter space remaining for normal ordering is progressively diminishing. Several proposals have been made to alleviate this tension, including neutrino decays [8–14], time-varying neutrino masses [15–19], additional interactions of neutrinos [20–25], and the production of massless dark radiation from neutrinos [26–28].

Cosmological observables are also sensitive to the free-streaming properties of neutrinos and any interactions that impede this free-streaming behavior. In particular, some cosmological data show an intriguing preference of beyond-the-Standard Model (BSM) interactions mediated by a heavy mediator [29–45]. Such self-interactions have also been shown to alleviate cosmological discrepancies, such as the H_0 and S_8 tensions. For flavor-universal self-interactions, CMB and Large Scale Structure (LSS), including Lyman- α , hint at the existence of moderately self-interacting (MI) neutrinos [41, 43, 45]. For flavor-specific self-interactions, where only one or two neutrino

flavors participate, data also accommodate strong self-interaction (SI) among neutrinos with a statistical significance similar to that of Λ CDM model with the Planck CMB data alone [35, 37, 38]. Using the CMB data from ACT DR4 further increases the significance of this SI mode [39, 46].

However, BSM neutrino self-interactions are subject to stringent laboratory constraints, including meson decays and double beta decay experiments [47–60], as well as constraints from supernovae [61–67], high-energy astrophysical neutrino sources [68–71] and BBN [72, 73]. Consequently, flavor-universal neutrino self-interactions are strongly excluded [74, 75]. While flavor-specific self-interactions (particularly those involving only τ neutrinos) are less constrained [38, 39], the viable parameter space remains quite limited.

To address these seemingly irreconcilable requirements from cosmology and laboratory constraints, we present a novel mechanism where strongly interacting dark radiation (DR) masquerades as self-interacting neutrinos after BBN. In this scenario, active neutrinos resonantly convert into strongly self-interacting DR between the BBN and CMB epochs. Note that such neutrino conversion has been used previously to relax the cosmological neutrino mass bound [26–28] or to generate sub-MeV dark matter [76–79]. However, the self-interacting DR playing the role of either flavor-specific or flavor-universal self-interacting neutrinos in this context has not been studied before.

After the neutrino-DR conversion is complete, the residual N_{eff} from neutrinos becomes (see Supplemental Section A)

$$N_{\text{eff}}^\nu \simeq N_{\text{eff}}^{\text{tot}} \frac{g_\nu}{g_\nu + g_\chi}, \quad (1)$$

where $g_\nu = \frac{7}{8} \times 2 \times 3$ represents the neutrino degrees of freedom (dof), $g_\chi = \frac{7}{8} \times 2 \times n_\chi$ denotes the DR dof, where n_χ is the number of flavors of χ . We achieve this via a Type-I seesaw-motivated model augmented by a scalar and massless DR, with the former coupled to the heavy sterile neutrinos. As shown in Eq. (1), thermalization between neutrinos and DR reduces neutrino energy density, thus relaxing the cosmological neutrino mass constraint. Furthermore, the same interaction that produces the DR also makes the DR strongly self-interacting, which, to cosmological observables, appears identical to self-interacting neutrinos. Lastly, the active neutrinos have negligible non-standard interactions at late times and are thus free from the laboratory constraints.

THE MECHANISM

Here we provide a proof-of-principle gauge-invariant model based on the Type-I seesaw mechanism for neutrino mass generation [80–84], where three generations

of left-handed Majorana sterile neutrinos N^c [85] are introduced to mediate between the SM and the dark sector (DS) via neutrino-Higgs Yukawa interactions

$$\mathcal{L} \supset \left(y^{\alpha i} L_\alpha N_i^c H - \frac{1}{2} M_N^{ii} N_i^c N_i^c + \text{h.c.} \right) + \mathcal{L}_{\text{dark}}. \quad (2)$$

Here, $\alpha = e, \mu, \tau$ denotes lepton flavor and $i = 1, 2, 3$ labels the sterile neutrino generations. Lepton number is explicitly broken by the Majorana mass term of N^c . After electroweak symmetry breaking, the Higgs vacuum expectation value v_H introduces a Dirac mass between the left-handed neutrinos ν_α and N^c with a mass matrix $m_D^{\alpha i} \equiv y^{\alpha i} v_H / \sqrt{2}$. In the seesaw limit $\mathbf{m}_D \ll \mathbf{M}_N$, the mixing between the interacting states $\{\nu_\alpha, N_i^c\}$ and the mass eigenstates $\{\nu_l, \nu_h\}$ is approximately given by [86]

$$\begin{aligned} \nu_\alpha &\approx U_{\alpha j} \left(\nu_l + i \sqrt{\mathbf{M}_N^{-1} \mathbf{m}_\nu} \nu_h \right)_j, \\ N_j^c &\approx \left(\nu_h - i \sqrt{\mathbf{M}_N^{-1} \mathbf{m}_\nu} \nu_l \right)_j, \end{aligned} \quad (3)$$

where $U_{\alpha j}$ is the PMNS matrix and \mathbf{m}_ν (\mathbf{M}_N) is the diagonal light (heavy) neutrino mass matrix.

The DS $\mathcal{L}_{\text{dark}}$ consists of a massive scalar ϕ and massless fermion(s) χ :

$$\mathcal{L}_{\text{dark}} \supset -\frac{1}{2} \lambda_{\phi N} \phi N_i^c N_i^c - \frac{1}{2} \lambda_{\phi \chi} \phi \chi^2 + \text{h.c.}, \quad (4)$$

where the couplings $\lambda_{\phi N}, \lambda_{\phi \chi}$ are chosen to be real without loss of generality. The small admixture of ν_l in N^c generates interactions between active neutrinos ν_l and the scalar ϕ with a coupling given by

$$\lambda_{\phi \nu} \approx \lambda_{\phi N} \frac{m_\nu}{M_N}. \quad (5)$$

Assuming the hierarchy $M_N \gtrsim \mathcal{O}(\text{MeV}) \gg m_\phi \gg m_\nu$, $\lambda_{\phi \nu}$ is typically $\sim 10^{-9}$ for our benchmark parameters, ensuring compatibility with laboratory bounds (see Supplemental Section B) while allowing for efficient cosmological effects. The equilibration of ν - χ can occur via the s -channel $\nu_l \nu_l \rightarrow \phi \rightarrow \chi \chi$, and the t -channel $\nu_l \nu_l \rightarrow \phi \phi$ followed by the immediate $\phi \rightarrow \chi \chi$ decay. Additionally, an $\mathcal{O}(1)$ $\lambda_{\phi \chi}$ allows for large self-interaction among the χ particles mediated by ϕ . When the temperature is much below the ϕ mass, the DR χ 's self-interaction term assumes the form of an effective 4-Fermi operator¹ $\frac{1}{4} G_{\text{eff}} (\chi \chi + \chi^\dagger \chi^\dagger)^2$ where

$$G_{\text{eff}} \equiv \frac{\lambda_{\phi \chi}^2}{m_\phi^2} \sim \frac{0.01}{\text{MeV}^2} \left(\frac{0.01 \text{MeV}}{m_\phi} \right)^2 \left(\frac{\lambda_{\phi \chi}}{10^{-3}} \right)^2. \quad (6)$$

¹ Such a choice reads $G_{\text{eff}} (\frac{1}{2} \bar{\Psi}_\chi \Psi_\chi) (\frac{1}{2} \bar{\Psi}_\chi \Psi_\chi)$ in the equivalent 4-component spinor representation where $\Psi_\chi \equiv (\chi \chi^\dagger)^T$.

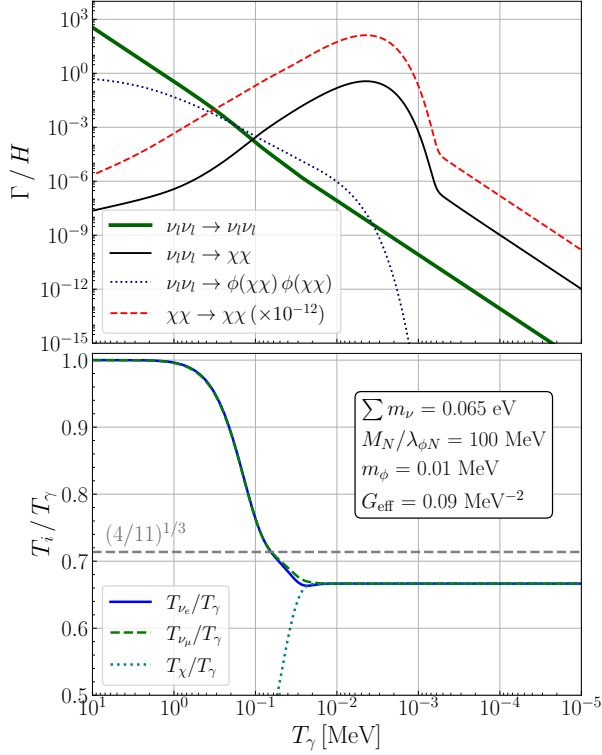


FIG. 1: Evolution of interaction rates (top) and temperatures (bottom) for a benchmark point with degenerate neutrino masses. The resonant $\nu - \chi$ conversion occurs when $T_\nu \sim m_\phi$, leading to efficient neutrino cooling (i.e. final $N_{\text{eff}}^\nu = 2.28$, $N_{\text{eff}}^{\text{tot}} = 3.04$).

To illustrate how active neutrino energy is transferred to dark radiation, and thus achieving Eq. (1), we plot evolutions of thermally averaged interaction rates (see Supplemental Section C) and temperatures for a benchmark model with $m_\phi = 0.01$ MeV, $M_N/\lambda_{\phi N} = 100$ MeV, $\sum m_\nu = 0.065$ eV and $G_{\text{eff}} = 0.09$ MeV $^{-2}$ in Fig. 1 assuming degenerate neutrino masses². Clearly, the t -channel process dominates the “freeze-in” of χ at early times when the bath temperature T_γ is higher than the mediator mass m_ϕ . Afterward, the s -channel process becomes resonantly enhanced when $T_\nu \simeq m_\phi$, resulting in an efficient conversion of SM neutrinos into the DR χ , thus cooling the neutrinos. This is reflected in the rapid drop of T_ν when $T_\nu \simeq m_\phi$. For the chosen benchmark, we obtain $N_{\text{eff}}^{\text{tot}} = 3.04$ after equilibration of ν and χ , with contribution from neutrinos given by $N_{\text{eff}}^\nu = 2.28$.

After χ kinetically decouples from ν , it maintains the same temperature as ν but exhibits a much stronger self-interaction, since for the chosen benchmark $\lambda_{\phi\nu}^2/\lambda_{\phi\chi}^2 \sim$

$m_\nu^2 / \left((M_N/\lambda_{\phi N})^2 G_{\text{eff}} m_\phi^2 \right) \sim 10^{-15}$. This benchmark successfully reproduces a flavor-specific self-interacting neutrino cosmology where 1/4 of active neutrinos having a self-interaction strength given by $G_{\text{eff}} = 0.09$ MeV $^{-2}$.

To demonstrate that neutrino cooling can be realized in this model generically, we solve Boltzmann equations varying the total neutrino mass $\sum m_\nu$ and the mediator mass m_ϕ (see Supplemental Section C) with $\lambda_{\phi\chi} = 0.003$, $M_N/\lambda_{\phi N} = 100$ MeV. The resultant N_{eff}^ν at $T_\gamma \sim 10^{-4}$ MeV, after $\chi - \nu$ decoupling, is shown in Fig. 2. It is clear that for a large parameter space, the equilibration happens in time where neutrinos are maximally cooled, i.e. $(N_{\text{eff}}^\nu = 3(1 + n_\chi/3)^{-1})$. When $n_\chi = 1$ (2), neutrinos together with DR behave as if 1/4 (2/5) of active neutrinos have significant self-interaction. One can convert more fractions of active neutrinos into self-interacting DR by increasing n_χ (see Supplemental Section C). When $n_\chi \gtrsim 40$, the neutrino contribution to N_{eff} is drastically reduced to $N_{\text{eff}}^\nu \lesssim 0.2$, with self-interacting DR constituting almost all $N_{\text{eff}}^{\text{tot}}$. This will mimic the flavor-universal neutrino self-interaction.

COSMOLOGICAL PHENOMENOLOGY

Having established that the model indeed allows for sufficient cooling of neutrinos, we now examine how this mechanism manifests in cosmological observations.

We perform a Bayesian analysis of the cosmological impact of our model with Planck-2018 dataset (temperature, polarization, and lensing) [87, 88] and DESI year-I data [89]. We focus on two scenarios, assuming one or two flavors of χ with maximal neutrino cooling (cf. Fig. 2). These two benchmarks are cosmologically equivalent to flavor-specific neutrino self-interactions, whereas we comment on flavor-universal interactions later. From Eq. (1), when the thermalization of $\nu - \chi$ is efficient, their contributions to N_{eff} after equilibration are given by³

$$(N_\chi, N_\nu) = \begin{cases} (0.75, 2.25) & \text{for } n_\chi = 1 \\ (1.20, 1.80) & \text{for } n_\chi = 2 \end{cases} \quad (7)$$

In the cosmological analysis N_ν neutrinos are free-streaming and N_χ dark radiations are self-interacting with the self-interaction rate of $\Gamma_\chi \propto G_{\text{eff}}^2 T_\chi^5$. The details of the cosmological analysis are given in the Supplemental Section D. In Fig. 3 and Table I, we summarize the results.

In Fig. 3 we show the triangle plot for $\log_{10}(G_{\text{eff}})$ and $\sum m_\nu$ from the Planck + DESI dataset for

² The mass hierarchy of neutrinos have negligible effect in the overall cooling of ν s. Benchmarks for normal ordering are shown in Supplemental Section C.

³ N_χ and N_ν are abbreviations of the effective number of dof N_{eff}^χ and N_{eff}^ν , respectively. In the cosmological analysis, we fixed the total $N_{\text{eff}}^{\text{tot}} = 3.044$ from NLO calculations [90]. For brevity we treat $N_{\text{eff}}^{\text{tot}} = 3$ for the notations in the paper.

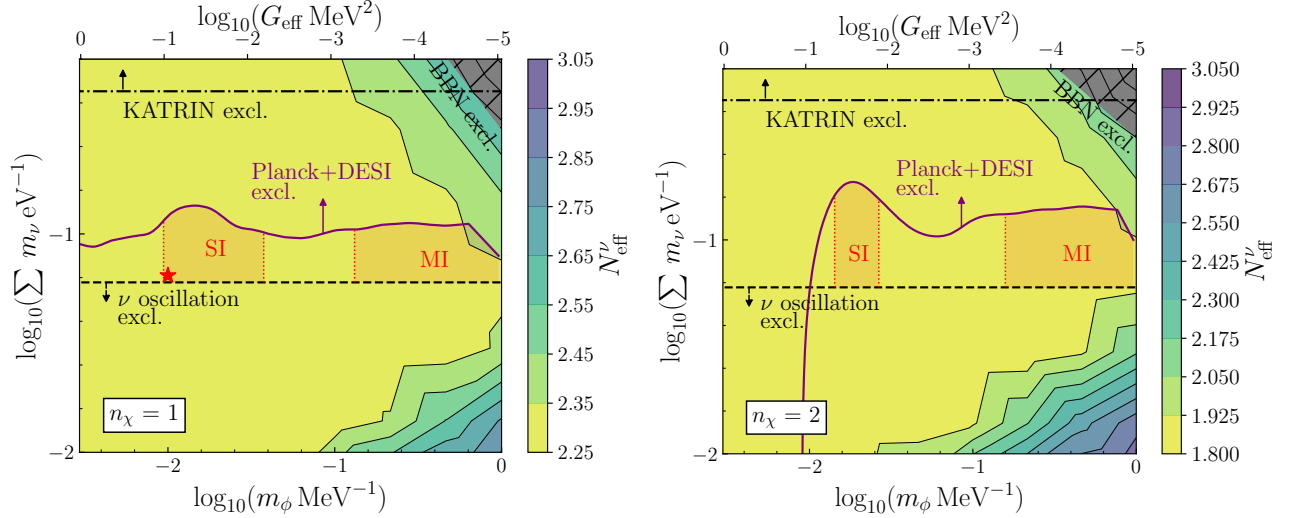


FIG. 2: ($\sum m_\nu, m_\phi$) plane for one (Left) and two (Right) flavors of DR with $\lambda_{\phi\chi} = 0.003$, $M_N/\lambda_{\phi N} = 100$ MeV assuming degenerate m_ν . The colored contours show N_{eff}^ν at $T_\gamma \sim 10^{-4}$ MeV. The upper right corner (gray hatched) is excluded by BBN where $\Delta N_{\text{eff}}^{\text{tot}} > 0.4$. Terrestrial neutrino mass bounds from ν oscillation (black dashed) and KATRIN (black dot-dashed) are overlaid. Magenta contours show the marginalized 2σ upper limit on $\sum m_\nu$ as a function of G_{eff} from Fig. 3. 1σ cosmological preferred SI and MI modes from Table I are shown in red bands in the region not excluded by ν oscillation and cosmology. The red star is the benchmark point used in Fig. 1.

a Nested sampling analysis of the entire parameter space. The 1D posterior of $\log_{10}(G_{\text{eff}} \text{MeV}^2)$ shows two distinct modes: the SI (strongly interacting) mode ($\log_{10}(G_{\text{eff}} \text{MeV}^2) \approx -2$) and the MI (moderately interacting) mode ($\log_{10}(G_{\text{eff}} \text{MeV}^2) \approx -4$). The SI mode is largely preferred over the MI mode, which can be seen from the 1D posterior. It is evident that the combined dataset favors cooler neutrinos and strongly self-interacting DR.

To quantify the preference of the SI mode, we performed a separate set of analyses restricting $\log_{10}(G_{\text{eff}} \text{MeV}^2)$ to the MI and SI regions by the following choice of priors on $\log_{10}(G_{\text{eff}} \text{MeV}^2)$: $[-5, -2.5]$ and $[-2.5, 0.0]$, respectively. Table I shows the relevant parameter limits (marginalized) and χ^2 comparison for Planck and Planck + DESI datasets. The χ^2 comparison shows that the SI mode is preferred over the MI mode for Planck + DESI dataset which exhibits the preference for strong neutrino interaction for the combined dataset.

Relaxation of neutrino mass bound

The 2D marginalized contours from Fig. 3 show a large relaxation of the upper limit of $\sum m_\nu$. In this mechanism, various effects lead to the relaxation of the neutrino mass bound. Conversion of massive neutrinos to massless χ reduces the effects of neutrino mass on cosmological observables due to a decrease in neutrino number density [26–28]. Using Eq. (1), the amount of the

relaxation can be computed as [28],

$$\sum m_\nu^{(N_\chi, N_\nu)} < \sum m_\nu^{(\Lambda\text{CDM})} \left(1 + \frac{N_\chi}{3} \right). \quad (8)$$

Here $\sum m_\nu^{(N_\chi, N_\nu)}$ is the bound in this cosmology and $\sum m_\nu^{(\Lambda\text{CDM})}$ is the bound in ΛCDM cosmology ($N_\nu = 3, N_\chi = 0$) with massive neutrinos. This is the primary mechanism for the relaxation of the neutrino mass bound in the MI region. In the SI mode region, there is additional relaxation of the neutrino mass. Large values of G_{eff} enhances DR density perturbation which amplifies the CMB spectra at small scale similar to the SI mode in neutrino self-interaction [33]. This enhancement is partially compensated by increasing the neutrino mass. This effect leads to further relaxation of the SI mode mass bound as shown in Fig. 3. Specifically, our model allows $\sum m_\nu$ up to 0.149 eV (0.385 eV) for the SI mode with Planck+DESI (Planck only) datasets.

Combined parameter space

In the $\sum m_\nu$ - m_ϕ plane (Fig. 2), we overlay the regions favored by cosmological data and those constrained by terrestrial and cosmological probes over the N_{eff}^ν contours. For a fixed value of $\lambda_{\phi\chi}$, the m_ϕ can be mapped to a value of G_{eff} following Eq. (6). We overlay the 2σ contour (magenta) from Fig. 3 which denotes the marginalized 2σ upper limit on $\sum m_\nu$ as a function of G_{eff} . With reference to terrestrial experiments, we also

N_{eff}	Mode	Planck			Planck+DESI		
		$\sum m_\nu$ [eV]	$\log_{10}(G_{\text{eff}} \text{ MeV}^2)$	$\Delta\chi^2$	$\sum m_\nu$ [eV]	$\log_{10}(G_{\text{eff}} \text{ MeV}^2)$	$\Delta\chi^2$
$0.75N_\chi + 2.25N_\nu$	MI	< 0.302	< -3.34	-3.36	< 0.104	< -3.28	-0.74
	SI	< 0.290	< -1.23	-0.26	< 0.114	$-1.27^{+0.28}_{-0.92}$	-1.34
$1.20N_\chi + 1.80N_\nu$	MI	< 0.392	< -3.48	-0.78	< 0.129	< -3.44	-0.34
	SI	< 0.385	$-1.66^{+0.34}_{-0.24}$	-0.38	< 0.149	$-1.65^{+0.30}_{-0.24}$	-1.66

TABLE I: 1σ constraints on the interaction parameter and 2σ upper bound on the sum of neutrino masses for the separate SI and MI mode analyses. We also show the χ^2 improvement of each mode over ΛCDM (with varying neutrino mass) for Planck and Planck+DESI datasets.

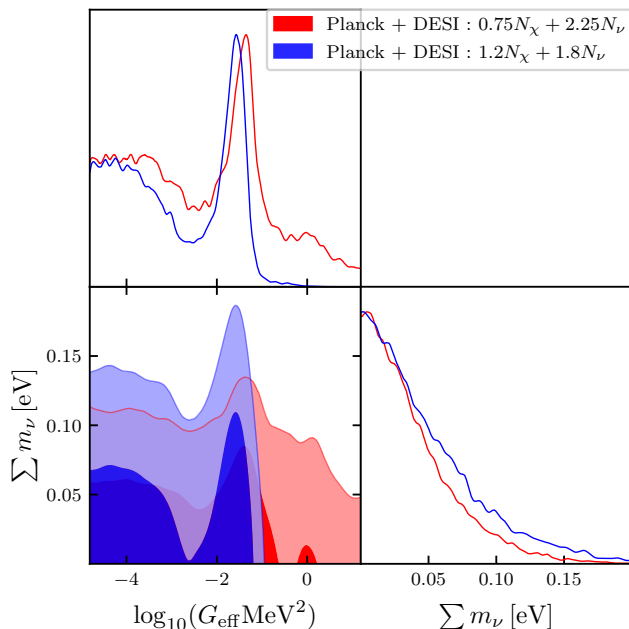


FIG. 3: 1D marginalized posterior and 2D marginalized contours for $\log_{10} G_{\text{eff}}$ and $\sum m_\nu$ with Planck + DESI dataset for $0.75N_\chi$ and $1.2N_\chi$ scenarios. The darker and lighter bands in 2D plot represent 1σ and 2σ allowed regions, respectively.

show the minimum $\sum m_\nu \geq 0.059$ eV (black dashed) from the oscillation data [1] and the latest upper bound of $\sum m_\nu < 0.45$ eV (dot-dashed) from KATRIN [2]. We show the 1σ ranges of cosmologically preferred SI and MI regions in red bands from Table I. Note that, for the choice of fixed parameters, both SI and MI regions lie in the parameter space of efficient conversion (yellow region) and showcase *viable* parameter space where neutrino mass is relaxed. Additionally, the SI region is cosmologically preferred over ΛCDM which corresponds to the limit $\log_{10}(G_{\text{eff}} \text{ MeV}^2) \lesssim -5$.

Flavor-universal self-interactions

So far, we have discussed how to reproduce the flavor-specific self-interaction scenario with DR. In the limit of large DR flavors, for instance, $n_\chi \gtrsim 40$, the active neutrino number density is drastically reduced: $N_\nu \lesssim 0.2$. Meanwhile, self-interacting DR number density increases: $N_\chi \gtrsim 2.8$, contributing to almost all of the $N_{\text{eff}}^{\text{tot}}$. This scenario mimics flavor-universal neutrino self-interactions, with the role of neutrinos played by DR. Due to very low neutrino number density, the neutrino mass constraint from cosmological analysis is significantly relaxed in this case (see Eq. (8)), which is within the reach of future direct search experiments like Project 8 [4] or even KATRIN [3]. Although the SI mode in flavor-universal interactions is not favored by CMB and LSS data, the MI mode is allowed by data at a large significance [36, 43, 45]. In our framework, both SI and MI modes can be realized free from those constraints (see Supplemental Section C).

CONCLUSION

This work highlights a broader paradigm in neutrino cosmology, where the degeneracy between neutrinos and neutrino-like dark radiation opens up new avenues for addressing cosmological tensions while respecting BBN and terrestrial constraints. We demonstrated this with a simple Type-I seesaw framework which provides a neutrino-mediator coupling that is weak enough to evade current laboratory bounds while impacting cosmology effectively via a strongly self-interacting dark sector. Future precision measurements of the high- ℓ CMB modes [39], LSS, and 21-cm probes [91], as well as laboratory searches for absolute neutrino mass [3, 4] and sterile neutrinos [92], will be crucial for distinguishing conventional neutrinos from such self-interacting dark sector scenarios.

ACKNOWLEDGMENTS

We would like to thank Nikita Blinov, Kimberly Boddy, Bhaskar Dutta, David Imig, Jessie Shelton, and

Yuhsin Tsai for useful discussions. This work used the high-performance computing service at the University of Notre Dame, managed by the Center for Research Computing (CRC) (<https://crc.nd.edu>). The authors acknowledge the Texas Advanced Computing Center (TACC) at The University of Texas at Austin for providing computational resources that have contributed to the research results reported within this paper (URL: <http://www.tacc.utexas.edu>). AD was supported by the Government of India DAE project No. RSI 4001. The work of BD was partly supported by the U.S. Department of Energy under grant No. DE-SC0017987, and by a Humboldt Fellowship from the Alexander von Humboldt Foundation. SG acknowledges support from the NSF under Grant No. PHY-2413016.

* anirban.das@saha.ac.in

† bdev@wustl.edu

‡ gaoy3@sustech.edu.cn

§ sghosh@utexas.edu

¶ tkim12@alumni.nd.edu

- [1] I. Esteban, M.C. Gonzalez-Garcia, M. Maltoni, I. Martinez-Soler, J.a.P. Pinheiro and T. Schwetz, *NuFit-6.0: updated global analysis of three-flavor neutrino oscillations*, *JHEP* **12** (2024) 216 [[2410.05380](#)].
- [2] KATRIN collaboration, *Direct neutrino-mass measurement based on 259 days of KATRIN data*, *Science* **388** (2025) adq9592 [[2406.13516](#)].
- [3] KATRIN collaboration, *KATRIN: status and prospects for the neutrino mass and beyond*, *J. Phys. G* **49** (2022) 100501 [[2203.08059](#)].
- [4] PROJECT 8 collaboration, *The Project 8 Neutrino Mass Experiment*, in *Snowmass 2021*, 3, 2022 [[2203.07349](#)].
- [5] J. Lesgourgues and S. Pastor, *Massive neutrinos and cosmology*, *Phys. Rept.* **429** (2006) 307 [[astro-ph/0603494](#)].
- [6] PLANCK collaboration, *Planck 2018 results. VI. Cosmological parameters*, *Astron. Astrophys.* **641** (2020) A6 [[1807.06209](#)].
- [7] DESI collaboration, *Constraints on Neutrino Physics from DESI DR2 BAO and DR1 Full Shape*, [2503.14744](#).
- [8] J.L. Aalberts et al., *Precision constraints on radiative neutrino decay with CMB spectral distortion*, *Phys. Rev. D* **98** (2018) 023001 [[1803.00588](#)].
- [9] Z. Chacko, A. Dev, P. Du, V. Poulin and Y. Tsai, *Cosmological Limits on the Neutrino Mass and Lifetime*, *JHEP* **04** (2020) 020 [[1909.05275](#)].
- [10] Z. Chacko, A. Dev, P. Du, V. Poulin and Y. Tsai, *Determining the Neutrino Lifetime from Cosmology*, *Phys. Rev. D* **103** (2021) 043519 [[2002.08401](#)].
- [11] M. Escudero, J. Lopez-Pavon, N. Rius and S. Sandner, *Relaxing Cosmological Neutrino Mass Bounds with Unstable Neutrinos*, *JHEP* **12** (2020) 119 [[2007.04994](#)].
- [12] G. Barenboim, J.Z. Chen, S. Hannestad, I.M. Oldengott, T. Tram and Y.Y.Y. Wong, *Invisible neutrino decay in precision cosmology*, *JCAP* **03** (2021) 087 [[2011.01502](#)].
- [13] G. Franco Abellán, Z. Chacko, A. Dev, P. Du, V. Poulin and Y. Tsai, *Improved cosmological constraints on the neutrino mass and lifetime*, *JHEP* **08** (2022) 076 [[2112.13862](#)].
- [14] J.Z. Chen, I.M. Oldengott, G. Pierobon and Y.Y.Y. Wong, *Weaker yet again: mass spectrum-consistent cosmological constraints on the neutrino lifetime*, *Eur. Phys. J. C* **82** (2022) 640 [[2203.09075](#)].
- [15] R. Fardon, A.E. Nelson and N. Weiner, *Dark energy from mass varying neutrinos*, *JCAP* **10** (2004) 005 [[astro-ph/0309800](#)].
- [16] C.S. Lorenz, L. Funcke, E. Calabrese and S. Hannestad, *Time-varying neutrino mass from a supercooled phase transition: current cosmological constraints and impact on the Ω_m - σ_8 plane*, *Phys. Rev. D* **99** (2019) 023501 [[1811.01991](#)].
- [17] C.S. Lorenz, L. Funcke, M. Löffler and E. Calabrese, *Reconstruction of the neutrino mass as a function of redshift*, *Phys. Rev. D* **104** (2021) 123518 [[2102.13618](#)].
- [18] M. Sen and A.Y. Smirnov, *Refractive neutrino masses, ultratight dark matter and cosmology*, *JCAP* **01** (2024) 040 [[2306.15718](#)].
- [19] M. Sen and A.Y. Smirnov, *Neutrinos with refractive masses and the DESI baryon acoustic oscillation results*, *Phys. Rev. D* **111** (2025) 103048 [[2407.02462](#)].
- [20] H.-J. He, Y.-Z. Ma and J. Zheng, *Resolving Hubble Tension by Self-Interacting Neutrinos with Dirac Seesaw*, *JCAP* **11** (2020) 003 [[2003.12057](#)].
- [21] M. Berbig, S. Jana and A. Trautner, *The Hubble tension and a renormalizable model of gauged neutrino self-interactions*, *Phys. Rev. D* **102** (2020) 115008 [[2004.13039](#)].
- [22] I. Esteban and J. Salvado, *Long Range Interactions in Cosmology: Implications for Neutrinos*, *JCAP* **05** (2021) 036 [[2101.05804](#)].
- [23] D. Green, D.E. Kaplan and S. Rajendran, *Neutrino interactions in the late universe*, *JHEP* **11** (2021) 162 [[2108.06928](#)].
- [24] I. Esteban, O. Mena and J. Salvado, *Nonstandard neutrino cosmology dilutes the lensing anomaly*, *Phys. Rev. D* **106** (2022) 083516 [[2202.04656](#)].
- [25] S. Foroughi-Abari, K.J. Kelly, M. Rai and Y. Zhang, *Enabling Strong Neutrino Self-Interaction with an Unparticle Mediator*, *Phys. Rev. Lett.* **134** (2025) 181001 [[2501.02049](#)].
- [26] J.F. Beacom, N.F. Bell and S. Dodelson, *Neutrinoless universe*, *Phys. Rev. Lett.* **93** (2004) 121302 [[astro-ph/0404585](#)].
- [27] Y. Farzan and S. Hannestad, *Neutrinos secretly converting to lighter particles to please both KATRIN and the cosmos*, *JCAP* **02** (2016) 058 [[1510.02201](#)].
- [28] M. Escudero, T. Schwetz and J. Terol-Calvo, *A seesaw model for large neutrino masses in concordance with cosmology*, *JHEP* **02** (2023) 142 [[2211.01729](#)].
- [29] F.-Y. Cyr-Racine and K. Sigurdson, *Limits on Neutrino-Neutrino Scattering in the Early Universe*, *Phys. Rev. D* **90** (2014) 123533 [[1306.1536](#)].
- [30] I.M. Oldengott, C. Rampf and Y.Y.Y. Wong, *Boltzmann hierarchy for interacting neutrinos I: formalism*, *JCAP* **04** (2015) 016 [[1409.1577](#)].

- [31] L. Lancaster, F.-Y. Cyr-Racine, L. Knox and Z. Pan, *A tale of two modes: Neutrino free-streaming in the early universe*, *JCAP* **07** (2017) 033 [[1704.06657](#)].
- [32] I.M. Oldengott, T. Tram, C. Rampf and Y.Y.Y. Wong, *Interacting neutrinos in cosmology: exact description and constraints*, *JCAP* **11** (2017) 027 [[1706.02123](#)].
- [33] C.D. Kreisch, F.-Y. Cyr-Racine and O. Doré, *Neutrino puzzle: Anomalies, interactions, and cosmological tensions*, *Phys. Rev. D* **101** (2020) 123505 [[1902.00534](#)].
- [34] S. Ghosh, R. Khatri and T.S. Roy, *Can dark neutrino interactions phase out the Hubble tension?*, *Phys. Rev. D* **102** (2020) 123544 [[1908.09843](#)].
- [35] A. Das and S. Ghosh, *Flavor-specific interaction favors strong neutrino self-coupling in the early universe*, *JCAP* **07** (2021) 038 [[2011.12315](#)].
- [36] S. Roy Choudhury, S. Hannestad and T. Tram, *Updated constraints on massive neutrino self-interactions from cosmology in light of the H_0 tension*, *JCAP* **03** (2021) 084 [[2012.07519](#)].
- [37] T. Brinckmann, J.H. Chang and M. LoVerde, *Self-interacting neutrinos, the Hubble parameter tension, and the cosmic microwave background*, *Phys. Rev. D* **104** (2021) 063523 [[2012.11830](#)].
- [38] S. Roy Choudhury, S. Hannestad and T. Tram, *Massive neutrino self-interactions and inflation*, *JCAP* **10** (2022) 018 [[2207.07142](#)].
- [39] A. Das and S. Ghosh, *The magnificent ACT of flavor-specific neutrino self-interaction*, *JCAP* **09** (2023) 042 [[2303.08843](#)].
- [40] J. Venzor, G. Garcia-Arroyo, J. De-Santiago and A. Pérez-Lorezana, *Resonant neutrino self-interactions and the H_0 tension*, *Phys. Rev. D* **108** (2023) 043536 [[2303.12792](#)].
- [41] D. Camarena, F.-Y. Cyr-Racine and J. Houghteling, *Confronting self-interacting neutrinos with the full shape of the galaxy power spectrum*, *Phys. Rev. D* **108** (2023) 103535 [[2309.03941](#)].
- [42] A. He, R. An, M.M. Ivanov and V. Gluscevic, *Self-interacting neutrinos in light of large-scale structure data*, *Phys. Rev. D* **109** (2024) 103527 [[2309.03956](#)].
- [43] A. Poudou, T. Simon, T. Montandon, E.M. Teixeira and V. Poulin, *Self-interacting neutrinos in light of recent CMB and LSS data*, **2503.10485**.
- [44] ACT collaboration, *The Atacama Cosmology Telescope: DR6 Constraints on Extended Cosmological Models*, **2503.14454**.
- [45] A. He, M.M. Ivanov, S. Bird, R. An and V. Gluscevic, *A Fresh Look at Neutrino Self-Interactions With the Lyman- α Forest: Constraints from EFT and PRIYA*, **2503.15592**.
- [46] C.D. Kreisch et al., *Atacama Cosmology Telescope: The persistence of neutrino self-interaction in cosmological measurements*, *Phys. Rev. D* **109** (2024) 043501 [[2207.03164](#)].
- [47] A.P. Lessa and O.L.G. Peres, *Revising limits on neutrino-Majoron couplings*, *Phys. Rev. D* **75** (2007) 094001 [[hep-ph/0701068](#)].
- [48] M. Agostini et al., *Results on $\beta\beta$ decay with emission of two neutrinos or Majorons in ^{76}Ge from GERDA Phase I*, *Eur. Phys. J. C* **75** (2015) 416 [[1501.02345](#)].
- [49] P.S. Pasquini and O.L.G. Peres, *Bounds on Neutrino-Scalar Yukawa Coupling*, *Phys. Rev. D* **93** (2016) 053007 [[1511.01811](#)].
- [50] K. Blum, Y. Nir and M. Shavit, *Neutrinoless double-beta decay with massive scalar emission*, *Phys. Lett. B* **785** (2018) 354 [[1802.08019](#)].
- [51] J.M. Berryman, A. De Gouvêa, K.J. Kelly and Y. Zhang, *Lepton-Number-Charged Scalars and Neutrino Beamstrahlung*, *Phys. Rev. D* **97** (2018) 075030 [[1802.00009](#)].
- [52] T. Brune and H. Päs, *Massive Majorons and constraints on the Majoron-neutrino coupling*, *Phys. Rev. D* **99** (2019) 096005 [[1808.08158](#)].
- [53] A. de Gouvêa, P.S.B. Dev, B. Dutta, T. Ghosh, T. Han and Y. Zhang, *Leptonic Scalars at the LHC*, *JHEP* **07** (2020) 142 [[1910.01132](#)].
- [54] V. Brdar, M. Lindner, S. Vogl and X.-J. Xu, *Revisiting neutrino self-interaction constraints from Z and τ decays*, *Phys. Rev. D* **101** (2020) 115001 [[2003.05339](#)].
- [55] PIENU collaboration, *Search for three body pion decays $\pi^+ \rightarrow l^+ \nu X$* , *Phys. Rev. D* **103** (2021) 052006 [[2101.07381](#)].
- [56] NA62 collaboration, *Search for K^+ decays to a muon and invisible particles*, *Phys. Lett. B* **816** (2021) 136259 [[2101.12304](#)].
- [57] S.A. Kharusi et al., *Search for Majoron-emitting modes of ^{136}Xe double beta decay with the complete EXO-200 dataset*, *Phys. Rev. D* **104** (2021) 112002 [[2109.01327](#)].
- [58] J.M. Berryman et al., *Neutrino self-interactions: A white paper*, *Phys. Dark Univ.* **42** (2023) 101267 [[2203.01955](#)].
- [59] P.S.B. Dev, D. Kim, D. Sathyan, K. Sinha and Y. Zhang, *New Laboratory Constraints on Neutrinophilic Mediators*, **2407.12738**.
- [60] Y. Zhang, *Neutrino Self-interaction and Weak Mixing Angle Measurements*, **2411.05070**.
- [61] A. Manohar, *A Limit on the Neutrino-neutrino Scattering Cross-section From the Supernova*, *Phys. Lett. B* **192** (1987) 217.
- [62] Y. Farzan, *Bounds on the coupling of the Majoron to light neutrinos from supernova cooling*, *Phys. Rev. D* **67** (2003) 073015 [[hep-ph/0211375](#)].
- [63] L. Heurtier and Y. Zhang, *Supernova Constraints on Massive (Pseudo)Scalar Coupling to Neutrinos*, *JCAP* **02** (2017) 042 [[1609.05882](#)].
- [64] A. Das, A. Dighe and M. Sen, *New effects of non-standard self-interactions of neutrinos in a supernova*, *JCAP* **05** (2017) 051 [[1705.00468](#)].
- [65] S. Shalgar, I. Tamborra and M. Bustamante, *Core-collapse supernovae stymie secret neutrino interactions*, *Phys. Rev. D* **103** (2021) 123008 [[1912.09115](#)].
- [66] P.-W. Chang, I. Esteban, J.F. Beacom, T.A. Thompson and C.M. Hirata, *Toward Powerful Probes of Neutrino Self-Interactions in Supernovae*, *Phys. Rev. Lett.* **131** (2023) 071002 [[2206.12426](#)].
- [67] D.F.G. Fiorillo, G.G. Raffelt and E. Vitagliano, *Strong Supernova 1987A Constraints on Bosons Decaying to Neutrinos*, *Phys. Rev. Lett.* **131** (2023) 021001 [[2209.11773](#)].
- [68] K. Ioka and K. Murase, *IceCube PeV–EeV neutrinos and secret interactions of neutrinos*, *PTEP* **2014** (2014) 061E01 [[1404.2279](#)].
- [69] K.C.Y. Ng and J.F. Beacom, *Cosmic neutrino cascades from secret neutrino interactions*, *Phys. Rev. D* **90** (2014) 065035 [[1404.2288](#)].

- [70] M. Bustamante, C. Rosenstrøm, S. Shalgar and I. Tamborra, *Bounds on secret neutrino interactions from high-energy astrophysical neutrinos*, *Phys. Rev. D* **101** (2020) 123024 [2001.04994].
- [71] I. Esteban, S. Pandey, V. Brdar and J.F. Beacom, *Probing secret interactions of astrophysical neutrinos in the high-statistics era*, *Phys. Rev. D* **104** (2021) 123014 [2107.13568].
- [72] G.-y. Huang, T. Ohlsson and S. Zhou, *Observational Constraints on Secret Neutrino Interactions from Big Bang Nucleosynthesis*, *Phys. Rev. D* **97** (2018) 075009 [1712.04792].
- [73] G.-y. Huang and W. Rodejohann, *Solving the Hubble tension without spoiling Big Bang Nucleosynthesis*, *Phys. Rev. D* **103** (2021) 123007 [2102.04280].
- [74] N. Blinov, K.J. Kelly, G.Z. Krnjaic and S.D. McDermott, *Constraining the Self-Interacting Neutrino Interpretation of the Hubble Tension*, *Phys. Rev. Lett.* **123** (2019) 191102 [1905.02727].
- [75] K.-F. Lyu, E. Stamou and L.-T. Wang, *Self-interacting neutrinos: Solution to Hubble tension versus experimental constraints*, *Phys. Rev. D* **103** (2021) 015004 [2004.10868].
- [76] A. Berlin and N. Blinov, *Thermal Dark Matter Below an MeV*, *Phys. Rev. Lett.* **120** (2018) 021801 [1706.07046].
- [77] A. Berlin and N. Blinov, *Thermal neutrino portal to sub-MeV dark matter*, *Phys. Rev. D* **99** (2019) 095030 [1807.04282].
- [78] D. Aloni, M. Joseph, M. Schmaltz and N. Weiner, *Dark Radiation from Neutrino Mixing after Big Bang Nucleosynthesis*, *Phys. Rev. Lett.* **131** (2023) 221001 [2301.10792].
- [79] C. Benso, T. Schwetz and D. Vatsyayan, *Large neutrino mass in cosmology and keV sterile neutrino dark matter from a dark sector*, *JCAP* **04** (2025) 054 [2410.23926].
- [80] P. Minkowski, $\mu \rightarrow e\gamma$ at a Rate of One Out of 10^9 Muon Decays?, *Phys. Lett. B* **67** (1977) 421.
- [81] R.N. Mohapatra and G. Senjanovic, *Neutrino Mass and Spontaneous Parity Nonconservation*, *Phys. Rev. Lett.* **44** (1980) 912.
- [82] T. Yanagida, *Horizontal gauge symmetry and masses of neutrinos*, *Conf. Proc. C* **7902131** (1979) 95.
- [83] M. Gell-Mann, P. Ramond and R. Slansky, *Complex Spinors and Unified Theories*, *Conf. Proc. C* **790927** (1979) 315 [1306.4669].
- [84] J. Schechter and J.W.F. Valle, *Neutrino Masses in $SU(2) \times U(1)$ Theories*, *Phys. Rev. D* **22** (1980) 2227.
- [85] A. de Gouvêa, *Neutrino Mass Models*, *Ann. Rev. Nucl. Part. Sci.* **66** (2016) 197.
- [86] J.A. Casas and A. Ibarra, *Oscillating neutrinos and $\mu \rightarrow e, \gamma$* , *Nucl. Phys. B* **618** (2001) 171 [hep-ph/0103065].
- [87] PLANCK collaboration, *Planck 2018 results. V. CMB power spectra and likelihoods*, *Astron. Astrophys.* **641** (2020) A5 [1907.12875].
- [88] PLANCK collaboration, *Planck 2018 results. VIII. Gravitational lensing*, *Astron. Astrophys.* **641** (2020) A8 [1807.06210].
- [89] DESI collaboration, *DESI 2024 VI: cosmological constraints from the measurements of baryon acoustic oscillations*, *JCAP* **02** (2025) 021 [2404.03002].
- [90] J.J. Bennett, G. Buldgen, P.F. De Salas, M. Drewes, S. Gariazzo, S. Pastor et al., *Towards a precision calculation of N_{eff} in the Standard Model II: Neutrino decoupling in the presence of flavour oscillations and finite-temperature QED*, *JCAP* **04** (2021) 073 [2012.02726].
- [91] S. Libanore, S. Ghosh, E.D. Kovetz, K.K. Boddy and A. Raccanelli, *Joint 21-cm and CMB Forecasts for Constraining Self-Interacting Massive Neutrinos*, **2504.15348**.
- [92] A.M. Abdullahi et al., *The present and future status of heavy neutral leptons*, *J. Phys. G* **50** (2023) 020501 [2203.08039].
- [93] L.C. Thomas, T. Dezen, E.B. Grohs and C.T. Kishimoto, *Electron-Positron Annihilation Freeze-Out in the Early Universe*, *Phys. Rev. D* **101** (2020) 063507 [1910.14050].
- [94] F.F. Deppisch, L. Graf, W. Rodejohann and X.-J. Xu, *Neutrino Self-Interactions and Double Beta Decay*, *Phys. Rev. D* **102** (2020) 051701 [2004.11919].
- [95] E.W. Kolb and M.S. Turner, *Supernova SN 1987a and the Secret Interactions of Neutrinos*, *Phys. Rev. D* **36** (1987) 2895.
- [96] D.F.G. Fiorillo, G.G. Raffelt and E. Vitagliano, *Large Neutrino Secret Interactions Have a Small Impact on Supernovae*, *Phys. Rev. Lett.* **132** (2024) 021002 [2307.15115].
- [97] PIENU collaboration, *Improved search for heavy neutrinos in the decay $\pi \rightarrow e\nu$* , *Phys. Rev. D* **97** (2018) 072012 [1712.03275].
- [98] NA62 collaboration, *Search for heavy neutral lepton production in K^+ decays to positrons*, *Phys. Lett. B* **807** (2020) 135599 [2005.09575].
- [99] GERDA collaboration, *Final Results of GERDA on the Search for Neutrinoless Double- β Decay*, *Phys. Rev. Lett.* **125** (2020) 252502 [2009.06079].
- [100] KAMLAND-ZEN collaboration, *Search for Majorana Neutrinos with the Complete KamLAND-Zen Dataset*, **2406.11438**.
- [101] P.D. Bolton, F.F. Deppisch and P.S.B. Dev, *Neutrinoless double beta decay versus other probes of heavy sterile neutrinos*, *JHEP* **03** (2020) 170 [1912.03058].
- [102] N. Sabti, A. Magalich and A. Filimonova, *An Extended Analysis of Heavy Neutral Leptons during Big Bang Nucleosynthesis*, *JCAP* **11** (2020) 056 [2006.07387].
- [103] A. Boyarsky, M. Ovchinnikov, O. Ruchayskiy and V. Syvolap, *Improved big bang nucleosynthesis constraints on heavy neutral leptons*, *Phys. Rev. D* **104** (2021) 023517 [2008.00749].
- [104] Y.-M. Chen and Y. Zhang, *BBN Constraint on Heavy Neutrino Production and Decay*, **2410.07343**.
- [105] A.D. Dolgov, S.H. Hansen and D.V. Semikoz, *Nonequilibrium corrections to the spectra of massless neutrinos in the early universe*, *Nucl. Phys. B* **503** (1997) 426 [hep-ph/9703315].
- [106] C.R. Harris et al., *Array programming with NumPy*, *Nature* **585** (2020) 357 [2006.10256].
- [107] P. Virtanen et al., *SciPy 1.0—Fundamental Algorithms for Scientific Computing in Python*, *Nature Meth.* **17** (2020) 261 [1907.10121].
- [108] V. Shtabovenko, R. Mertig and F. Orellana, *FeynCalc 10: Do multiloop integrals dream of computer codes?*, *Comput. Phys. Commun.* **306** (2025) 109357

- [2312.14089].
- [109] T. Hahn, *FeynArts 3.11 user's guide*, *Comput. Phys. Commun.* **140** (2001) 418 [[hep-ph/0012260](#)].
- [110] A. Alloul, N.D. Christensen, C. Degrande, C. Duhr and B. Fuks, *FeynRules 2.0 - A complete toolbox for tree-level phenomenology*, *Comput. Phys. Commun.* **185** (2014) 2250 [[1310.1921](#)].
- [111] P. Gondolo and G. Gelmini, *Cosmic abundances of stable particles: Improved analysis*, *Nucl. Phys. B* **360** (1991) 145.
- [112] C.-P. Ma and E. Bertschinger, *Cosmological perturbation theory in the synchronous and conformal Newtonian gauges*, *Astrophys. J.* **455** (1995) 7 [[astro-ph/9506072](#)].
- [113] T. Brinckmann, J.H. Chang, P. Du and M. LoVerde, *Confronting interacting dark radiation scenarios with cosmological data*, *Phys. Rev. D* **107** (2023) 123517 [[2212.13264](#)].
- [114] J. Lesgourgues, *The Cosmic Linear Anisotropy Solving System (CLASS) I: Overview*, [1104.2932](#).
- [115] D. Blas, J. Lesgourgues and T. Tram, *The Cosmic Linear Anisotropy Solving System (CLASS) II: Approximation schemes*, *JCAP* **07** (2011) 034 [[1104.2933](#)].
- [116] F. Feroz and M.P. Hobson, *Multimodal nested sampling: an efficient and robust alternative to MCMC methods for astronomical data analysis*, *Mon. Not. Roy. Astron. Soc.* **384** (2008) 449 [[0704.3704](#)].
- [117] F. Feroz, M.P. Hobson and M. Bridges, *MultiNest: an efficient and robust Bayesian inference tool for cosmology and particle physics*, *Mon. Not. Roy. Astron. Soc.* **398** (2009) 1601 [[0809.3437](#)].
- [118] F. Feroz, M.P. Hobson, E. Cameron and A.N. Pettitt, *Importance Nested Sampling and the MultiNest Algorithm*, *Open J. Astrophys.* **2** (2019) 10 [[1306.2144](#)].
- [119] J. Buchner, A. Georgakakis, K. Nandra, L. Hsu, C. Rangel, M. Brightman et al., *X-ray spectral modelling of the AGN obscuring region in the CDFS: Bayesian model selection and catalogue*, *Astron. Astrophys.* **564** (2014) A125 [[1402.0004](#)].
- [120] B. Audren, J. Lesgourgues, K. Benabed and S. Prunet, *Conservative Constraints on Early Cosmology: an illustration of the Monte Python cosmological parameter inference code*, *JCAP* **02** (2013) 001 [[1210.7183](#)].
- [121] T. Brinckmann and J. Lesgourgues, *MontePython 3: boosted MCMC sampler and other features*, *Phys. Dark Univ.* **24** (2019) 100260 [[1804.07261](#)].
- [122] L. Herold and M. Kamionkowski, *Revisiting the impact of neutrino mass hierarchies on neutrino mass constraints in light of recent DESI data*, *Phys. Rev. D* **111** (2025) 083518 [[2412.03546](#)].
- [123] DESI collaboration, *DESI DR2 Results II: Measurements of Baryon Acoustic Oscillations and Cosmological Constraints*, [2503.14738](#).
- [124] N. Metropolis, A.W. Rosenbluth, M.N. Rosenbluth, A.H. Teller and E. Teller, *Equation of state calculations by fast computing machines*, *J. Chem. Phys.* **21** (1953) 1087.
- [125] W.K. Hastings, *Monte Carlo Sampling Methods Using Markov Chains and Their Applications*, *Biometrika* **57** (1970) 97.

Supplemental Material

A. Neutrino Cooling from Interaction with Dark Sector

We focus on the period of cosmology after neutrino decoupling ($T \lesssim \text{MeV}$) and before photon decoupling ($T \gtrsim 0.2 \text{ eV}$). In the radiation-dominated era, the total energy density is given by

$$\rho_{\text{rad}} = \rho_{\gamma} \left[1 + \frac{7}{8} \left(\frac{T_{\nu}^{\text{SM}}}{T} \right)^4 N_{\text{eff}} \right], \quad (\text{S1})$$

where T is the photon temperature, and $\rho_{\gamma} = \frac{\pi^2}{15} T^4$. Here T_{ν}^{SM} is the same as T before electron-positron annihilation, but equal to $\left(\frac{4}{11}\right)^{1/3} T$ afterward.

1. Neutrino-DS Equilibrium

Before the DS is in equilibrium with the neutrino sector, it can have a different temperature. The process of two sectors with different temperatures coming into equilibrium does not conserve entropy, but conserves energy, i.e.,

$$(\rho_{\nu} + \rho_{\text{DS}}) a^4 = \text{constant}, \quad (\text{S2})$$

where $\rho_i = \frac{\pi^2}{30} g_i T_i^4 \times 1$ (or $7/8$) for bosons (or fermions). For notational simplicity, we absorb $7/8$ into the definition of g_i . Separately, the photon and electron bath (later the photon bath after electron-positron annihilation) has to conserve entropy, i.e.

$$g_{\gamma}(T) T^3 a^3 = \text{constant}. \quad (\text{S3})$$

Rescaling Eq. (S3) to cancel a in Eq. (S2), let us compare the time of neutrino decoupling T_i^0 and later the time of neutrino-DS equilibrium T_i^{eq} :

$$\frac{g_\nu(T_\nu^0)\xi_\nu^{04} + g_{\text{DS}}(T_{\text{DS}}^0)\xi_{\text{DS}}^{04}}{g_\gamma(T^0)^{4/3}} = \frac{(g_\nu(T_\nu^{\text{eq}}) + g_{\text{DS}}(T_\nu^{\text{eq}}))\xi_\nu^{\text{eq}4}}{g_\gamma(T^{\text{eq}})^{4/3}}, \quad (\text{S4})$$

where $\xi_i \equiv T_i/T$. Therefore,

$$\xi_\nu^{\text{eq}} = \left(\frac{g_\gamma(T^{\text{eq}})}{g_\gamma(T^0)} \right)^{1/3} \left(\frac{g_\nu(T_\nu^0)\xi_\nu^{04} + g_{\text{DS}}(T_{\text{DS}}^0)\xi_{\text{DS}}^{04}}{g_\nu(T_\nu^{\text{eq}}) + g_{\text{DS}}(T_{\text{DS}}^{\text{eq}})} \right)^{1/4}. \quad (\text{S5})$$

For the photon bath, depending on whether the neutrino-DS equilibrium happens before or after the electron-positron-annihilation decoupling from the bath which happens at $T^{e^+e^-} \approx 16$ keV [93], we have

$$\frac{g_\gamma(T^{\text{eq}})}{g_\gamma(T^0)} \approx \begin{cases} 1, & T^{\text{eq}} > T^{e^+e^-} \\ \frac{2}{\frac{7}{8} \times 4 + 2} = \frac{4}{11}, & T^{\text{eq}} < T^{e^+e^-} \end{cases}. \quad (\text{S6})$$

For the neutrino sector, g_ν remains constant and is given by $\frac{7}{8} \times 2 \times 3$.

For the DS, we assume that $\xi_{\text{DS}}^0 \ll 1$, and thus the DS is populated by interactions with light neutrinos only. After it reaches equilibrium with light neutrinos, $g_{\text{DS}}(T_{\text{DS}}^{\text{eq}}) = 1(\text{scalar mediator}) + \frac{7}{8} \times 2 \times n_{\text{DR}}(\text{Majorana fermions})$, where n_{DR} is the number of DR species for the model presented in the main text, cf. Eq. (4). With $\xi_\nu^{\text{SM}} = 1$ (or $(\frac{4}{11})^{1/3}$) before (or after) the electron position annihilation, we have

$$\xi_\nu^{\text{eq}} = \left(\frac{g_\nu}{g_\nu + g_{\text{DS}}(T_\nu^{\text{eq}})} \right)^{1/4} \xi_\nu^{\text{SM}}. \quad (\text{S7})$$

2. Decoupling of the Mediator

At a later time, the temperature drops well below the mediator mass and the scalar mediator decouples at around $T_\nu^{\phi \text{ dec}}$. This happens within the thermal bath of the neutrino-DS, thus the entropy is conserved within that sector:

$$[g_\nu(T_\nu) + g_{\text{DS}}(T_\nu)] T_\nu^3 a^3 = \text{constant}. \quad (\text{S8})$$

Again, using Eq. (S3) to cancel a , let us compare the time before and after ϕ decouples:

$$\frac{(g_\nu + g_{\text{DS}}(T_\nu^{\text{eq}}))\xi_\nu^{\text{eq}3}}{g_\gamma} = \frac{(g_\nu + g_{\text{DS}}(T_\nu^{\phi \text{ dec}}))\xi_\nu^{\phi \text{ dec}3}}{g_\gamma}. \quad (\text{S9})$$

where $g_\nu = \frac{7}{8} \times 2 \times 3$ remains constant. Thus,

$$\xi_\nu^{\phi \text{ dec}} = \left(\frac{g_\nu + g_{\text{DS}}(T_\nu^{\text{eq}})}{g_\nu + g_{\text{DS}}(T_\nu^{\phi \text{ dec}})} \right)^{1/3} \left(\frac{g_\nu}{g_\nu + g_{\text{DS}}(T_\nu^{\text{eq}})} \right)^{1/4} \xi_\nu^{\text{SM}}. \quad (\text{S10})$$

Since g_{DS} is going to decrease by 1 after ϕ decouples, we have $T_\nu^{\text{eq}} \leq T_\nu^{\phi \text{ dec}} < T_\nu^{\text{SM}}$.

Note that T_ν^{eq} can be equal to $T_\nu^{\phi \text{ dec}}$ if the ϕ decay rate is much larger than the Hubble rate, since under such circumstances ϕ would not be long-lived enough to be equilibrated within the thermal bath of the DS. The amount of final cooling of neutrinos is controlled by the number of DR species in the DS.

At an even later time, when the cross-section of $\nu\nu \rightarrow \chi\chi$ becomes small compared to the expansion rate, χ kinetically decouples from the neutrino sector again. Just like the story of neutrino decoupling from the SM, the χ particles behave as dark radiation and maintain the same temperature as the neutrinos.

3. N_{eff} from DS and neutrinos

After the DS and neutrinos become equilibrated, the total radiation becomes

$$\rho_{\text{rad}} = \rho_\gamma + \rho_\nu + \rho_{\text{DS}} = \rho_\gamma \left[1 + \frac{7}{8} \left(\frac{T_\nu^{\text{SM}}}{T} \right)^4 N_{\text{eff}}^{\text{SM}} \frac{g_\nu + g_{\text{DS}}}{g_\nu} \left(\frac{\xi_\nu}{\xi_\nu^{\text{SM}}} \right)^4 \right]. \quad (\text{S11})$$

Comparing with Eq. (S1), we have

$$N_{\text{eff}} = N_{\text{eff}}^{\text{SM}} \frac{g_\nu + g_{\text{DS}}}{g_\nu} \left(\frac{\xi_\nu}{\xi_\nu^{\text{SM}}} \right)^4. \quad (\text{S12})$$

After ϕ decouples, N_{eff} becomes

$$N_{\text{eff}}(T_\nu^{\phi \text{ dec}}) = N_{\text{eff}}^{\text{SM}} \left(\frac{g_\nu + g_{\text{DS}}(T_\nu^{\text{eq}})}{g_\nu + g_{\text{DS}}(T_\nu^{\phi \text{ dec}})} \right)^{4/3} \geq N_{\text{eff}}^{\text{SM}}. \quad (\text{S13})$$

The equal sign occurs if ϕ is very short-lived, thus having a negligible number density in the thermal bath of neutrino-DS. The neutrino's contribution to N_{eff} is thus

$$N_{\text{eff}}^\nu = N_{\text{eff}}(T_\nu^{\phi \text{ dec}}) \frac{g_\nu}{g_\nu + g_{\text{DS}}(T_\nu^{\phi \text{ dec}})}. \quad (\text{S14})$$

If ϕ is very short-lived, i.e. $T_\nu^{\phi \text{ dec}} \approx T_\nu^{\text{eq}}$,

$$N_{\text{eff}}^\nu \simeq N_{\text{eff}}^{\text{SM}} \frac{g_\nu}{g_\nu + g_{\text{DR}}} = N_{\text{eff}}^{\text{SM}} \frac{3}{3 + n_{\text{DR}}}, \quad (\text{S15})$$

where n_{DR} is the number of fermion DR flavors present in the DS. This completes the derivation of Eq. (1) given in the main text.

B. Laboratory and BBN Constraints

As summarized in Fig. 1 of Ref. [58], various cosmological, astrophysical, and laboratory constraints have ruled out neutrino-mediator couplings larger than approximately 10^{-7} when the mediator mass is below 1 MeV. For the mediator mass in the keV–MeV range, the constraints on the neutrino-mediator coupling mainly come from laboratory measurements such as double-beta decay ($\phi\beta\beta$) [48, 52, 57, 94] and the rare meson/ τ / Z decays [51, 54, 59], with the strongest bound coming from $\phi\beta\beta$ requiring $\lambda_{\nu_e\nu_e} \lesssim 10^{-5}$ [52]. Furthermore, there are astrophysical bounds from long-baseline observations, such as those of neutrinos from SN 1987A [65, 95, 96] which require $\lambda_{\nu_\alpha\nu_\alpha} \lesssim 10^{-2}$ assuming flavor-universal interactions. In our model, the neutrino-mediator coupling [cf. Eq. (5)] is approximately $\leq 10^{-9}$ for each neutrino mass eigenstate, and is consistent with the aforementioned constraints.

Additionally, our model introduces mixing between SM-like neutrinos and heavy sterile neutrinos, making bounds from laboratory searches for heavy neutral lepton (HNL) applicable. For M_N in the MeV range, precision measurements of meson decays [97, 98] and neutrinoless double beta decay searches [99, 100] can probe the active-sterile mixing angle [cf. Eq. (3)], which is approximately given by $m_\nu/M_N \lesssim 10^{-8}$ in our case. This extreme suppression arises naturally from the seesaw mechanism without any fine-tuning. Since we are not interested in the phenomenology of HNLs in this work, we have verified that our benchmark $M_N = 10$ MeV is consistent with all existing terrestrial constraints [101]. Nevertheless, future HNL searches in meson decays and beam dump experiments [92] could provide an important test of our model.

If the sterile neutrinos come into equilibrium prior to BBN and decay to DR, it may significantly affect N_{eff} and thus be severely constrained [102–104]. Such constraints can however be avoided by choosing a low reheating temperature. In Fig. S1, we show the rate over Hubble for dominant processes that keep the active neutrinos and the sterile neutrinos in the thermal bath with the SM particles. Sterile neutrino production happens through mixing with the active neutrino such as $e\nu_l \rightarrow e\nu_h$, or pair production via exchange of Z or ϕ in $\nu_l\nu_l \rightarrow \nu_h\nu_h$. First, $e(\nu_l)\nu_l \rightarrow e(\nu_l)\nu_h$ yields the same temperature dependence as the SM $e\nu_l \rightarrow e\nu_l$, but scaled down by m_{ν_l}/M_N with a minimum energy requirement factor $\sqrt{1 - M_N^2/s}$. Therefore, $e\nu_l \rightarrow e\nu_h$ (green) and $\nu_l\nu_l \rightarrow \nu_l\nu_h$ (blue) have the same

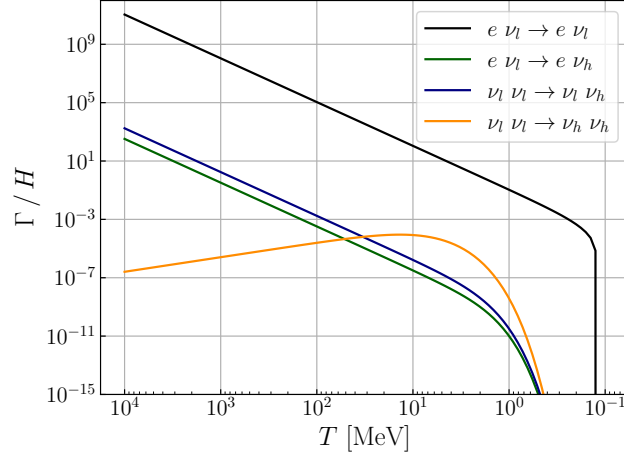


FIG. S1: Rate over Hubble for dominant processes that keep the active neutrinos and the sterile neutrinos (or HNLs) in the thermal bath with the SM particles. The production of HNL via $e(\nu_l)\nu_l \rightarrow e(\nu_l)\nu_h$ only depends on the mixing angle between active neutrinos and sterile neutrinos, hence, their rates (blue and green) scale down by $\sim m_{\nu_l}/M_N$ with respect to the SM $e\nu_l \rightarrow e\nu_l$ (black). HNL pair production via Z/ϕ as mediators has $\Gamma/H \lesssim 10^{-3}$ at any time. Therefore, requiring $\Gamma/H < 1$ for HNL production at all times implies a low-reheating temperature ($\lesssim 1$ GeV).

behavior as the SM (black). In addition, sterile neutrinos can be pair produced via exchange of Z and ϕ . Z mediated channel is suppressed at low energy, yet, the contribution rises as the temperature increases following the trend of $e - \nu$ scattering. On the other hand, ϕ exchange process comprises of all s -, t - and u -channel in cross-section [cf. Eq. (S32)], creating a long-tailed $\Gamma/H \sim T^{-1}$ behavior (orange). Estimates using Γ/H show that as long as the reheating temperature is approximately below 100 MeV–1 GeV, there is not enough time for the sterile neutrinos to equilibrate with the SM before BBN.

Unlike the model of strong neutrino self-interaction [74], the mediator ϕ in our model is not strongly constrained by BBN since the resonant conversion of neutrinos to DR takes place after BBN (before CMB) for the viable parameter space and the neutrino coupling to ϕ itself is tiny. If the conversion process takes place close to BBN ($m_\phi \sim \text{MeV}$), ΔN_{eff} can be significantly affected (cf. Fig. S3 below). This is reflected in the upper right corner of Fig. 2, which is excluded (gray hatched) since $\Delta N_{\text{eff}}^{\text{tot}} > 0.4$. There, thermalization of χ leads to cooling of all particles (e^\pm , γ) that are in the thermal bath. Since $N_{\text{eff}}^{\text{tot}}$ is a measure of radiation energy density other than photons over the photon energy density, efficient cooling of all species can lead to an overall increase of $N_{\text{eff}}^{\text{tot}}$.

C. Boltzmann Equations and Thermal History

In this section, we derive the thermal history of the modified cosmology in our model by solving the relevant Boltzmann equations.

1. Setting up the Boltzmann Equations

Our main interest is to monitor how the temperature of neutrinos evolves as the DR gets produced. In order to do so, we start from the homogeneous and isotropic Boltzmann equation with a collision term:

$$\frac{\partial f}{\partial t} - H p \frac{\partial f}{\partial p} = C[f], \quad (\text{S16})$$

where $f = f(t, p)$ is the distribution function. Assuming a Maxwell-Boltzmann distribution (which is a good approximation in the radiation-dominated epoch), the collision term is

$$C[f_1] = -\frac{1}{2E_1} \int d\Pi_2 d\Pi_3 d\Pi_4 \delta^{(4)}(p_1 + p_2 - p_3 - p_4) \times (|\mathcal{M}_{12 \rightarrow 34}|^2 f_1 f_2 - |\mathcal{M}_{34 \rightarrow 12}|^2 f_3 f_4), \quad (\text{S17})$$

where $d\Pi_n = \frac{d^3 p_n}{(2\pi)^3 2E_n}$ is the phase-space factor, and

$$|\mathcal{M}_{12 \rightarrow 34}|^2 = |\mathcal{M}_{34 \rightarrow 12}|^2 = \frac{1}{g_1} S \sum_{\text{spin}} |\mathcal{M}|^2. \quad (\text{S18})$$

Here $\sum_{\text{spin}} |\mathcal{M}|^2$ is summed over spins of all particles except the first one, g_i is the internal dof, and S is the symmetrization factor which includes $\frac{1}{2!}$ for each pair of identical particles in initial and final states and the factor 2 if there are 2 identical particles in the initial state [105].

We multiply both sides of Eq. (S16) by $\int g_1 E_1 \frac{d^3 p_1}{(2\pi)^3}$, and obtain an equation for the energy density evolution of particle 1:

$$\begin{aligned} \frac{d\rho_1}{dt} + 3H(\rho_1 + P_1) &= \int g_1 E_1 \frac{d^3 p_1}{(2\pi)^3} C[f_1] \\ &= - \int 2E_1 \left(\prod_{i=1}^4 d\Pi_i \right) (2\pi)^4 \delta^{(4)}(p_1 + p_2 - p_3 - p_4) \times \frac{S}{4} \sum_{\text{spin}} |\mathcal{M}|^2 (f_1 f_2 - f_3 f_4) \\ &= - \int \frac{d^3 p_1}{(2\pi)^3} \frac{d^3 p_2}{(2\pi)^3} 2E_1 \sigma v (f_1 f_2 - f_3 f_4) \equiv \frac{\delta\rho_{12 \rightarrow 34}}{\delta t}, \end{aligned} \quad (\text{S19})$$

where P_1 is the fluid pressure, σ is the cross-section, v is the Møller velocity, and the initial (final) state particles are assumed to be identical. Suppose that the initial (final) state particles have a temperature T (T'). The collision term can be further simplified as

$$\frac{\delta\rho_{12 \rightarrow 34}}{\delta t} = - \frac{S}{(2\pi)^4} \int_{s_{\min}}^{\infty} ds \sigma s^2 \left[TK_2\left(\frac{\sqrt{s}}{T}\right) - T' K_2\left(\frac{\sqrt{s}}{T'}\right) \right], \quad (\text{S20})$$

where s is the center-of-mass energy and K_2 is the modified Bessel function of the second kind. Furthermore, the right-hand-side of the Eq. (S19) needs to be a linear combination of all possible interactions that affect particle 1 except for the self-interaction. This accounts for all possible energy flows as a given particle type transfers into the other. For instance, in the ν_e sector, we may compartmentalize the total energy transfer term into SM-only term ($\frac{\delta\rho_{\nu_e}^{\text{SM}}}{\delta t}$) and new BSM terms ($\frac{\delta\rho_{\nu_e}^{\text{BSM}}}{\delta t}$). In temperature evolution equations (S21–S24) below, energy transfer of BSM is explicitly presented.

We are interested in the cosmological era from BBN to CMB during which the photon, neutrino and the DS may come out or reach equilibrium, i.e. their temperatures $T_\gamma, T_{\nu_e, \mu, \tau}, T_\chi$ may evolve separately. Assuming $T_{\nu_\tau} = T_{\nu_\mu}$, there will be four coupled temperature evolution ($\dot{T} \equiv dT/dt$) equations, which can be obtained from the Boltzmann equations for density evolution as follows:

$$\dot{T}_\gamma \left(\frac{\partial \rho_e}{\partial T_\gamma} + \frac{\partial \rho_\gamma}{\partial T_\gamma} \right) + 4H\rho_\gamma + 3H(\rho_e + P_e) = - \frac{\delta\rho_{\nu_e}}{\delta t} - 2 \frac{\delta\rho_{\nu_\mu}}{\delta t}, \quad (\text{S21})$$

$$\dot{T}_{\nu_e} \frac{\partial \rho_{\nu_e}}{\partial T_{\nu_e}} + 4H\rho_{\nu_e} = \frac{\delta\rho_{\nu_e \nu_e \rightarrow \chi\chi}}{\delta t} + \frac{\delta\rho_{\nu_e \nu_e \rightarrow 4\chi}}{\delta t} + \frac{\delta\rho_{\nu_e \nu_\mu \rightarrow 4\chi}}{\delta t} + \frac{\delta\rho_{\nu_e \nu_\mu \rightarrow \chi\chi}}{\delta t} + \frac{\delta\rho_{\nu_e}}{\delta t}, \quad (\text{S22})$$

$$\dot{T}_{\nu_\mu} \frac{\partial \rho_{\nu_\mu}}{\partial T_{\nu_\mu}} + 4H\rho_{\nu_\mu} = \frac{\delta\rho_{\nu_\mu \nu_\mu \rightarrow \chi\chi}}{\delta t} + \frac{\delta\rho_{\nu_\mu \nu_\mu \rightarrow 4\chi}}{\delta t} + \frac{\delta\rho_{\nu_e \nu_\mu \rightarrow 4\chi}}{\delta t} + \frac{\delta\rho_{\nu_e \nu_\mu \rightarrow \chi\chi}}{\delta t} + \frac{\delta\rho_{\nu_\mu}}{\delta t}, \quad (\text{S23})$$

$$\dot{T}_\chi \frac{\partial \rho_\chi}{\partial T_\chi} + 4H\rho_\chi = - \frac{\delta\rho_{\nu_e \nu_e \rightarrow 4\chi}}{\delta t} - 2 \frac{\delta\rho_{\nu_\mu \nu_\mu \rightarrow 4\chi}}{\delta t} - 3 \frac{\delta\rho_{\nu_e \nu_\mu \rightarrow 4\chi}}{\delta t} - \frac{\delta\rho_{\nu_e \nu_e \rightarrow \chi\chi}}{\delta t} - 2 \frac{\delta\rho_{\nu_\mu \nu_\mu \rightarrow \chi\chi}}{\delta t} - 3 \frac{\delta\rho_{\nu_e \nu_\mu \rightarrow \chi\chi}}{\delta t}. \quad (\text{S24})$$

Here the right hand sides are collision terms of different processes which are functions of temperatures only. Note that in our convention, $\frac{\delta\rho_{\nu_e}}{\delta t}$ is the energy transfer under the SM which receives contributions from $\nu_e \nu_e \leftrightarrow \nu_l \nu_l$, $\nu_e \nu_l \leftrightarrow \nu_e \nu_l$, $\nu_e e \leftrightarrow \nu_e e$, and $\nu_e \nu_e \leftrightarrow ee$ yielding the conventional neutrino decoupling in cosmology.

To obtain the left hand sides, we assume the form of ideal gases for each species and use the relation $\dot{\rho}_i = \frac{\partial \rho_i}{\partial T_i} \dot{T}_i$. Furthermore, H can be traded for ρ using the Friedmann equation $H^2 = \frac{8\pi G \rho_{\text{tot}}}{3}$, where $\rho_{\text{tot}} = \rho_\gamma + \rho_e + \rho_{\nu_e} + 2\rho_{\nu_\mu} + \rho_\chi$. It can be easily verified that the total energy is conserved i.e. $\dot{\rho}_{\text{tot}} = -3H(\rho_{\text{tot}} + P_{\text{tot}})$. Note that we did not include ϕ in the DS bath, since for the range of ϕ mass and the temperature of interest it decays immediately to χ . The boosted decay width $\Gamma_\phi E_\phi/m_\phi$ is much higher than the Hubble within our time range. Therefore, process of ϕ pair production is equivalent to the decay of $\phi \rightarrow \chi\chi$ assuming that the branching ratio of $\phi \rightarrow \nu\nu$ is suppressed by the $\nu - \phi$ coupling, $\lesssim 10^{-8}$, cf. Eq. (S27). The coupled differential equations (S21)–(S24) are numerically solved using python with numpy [106] and odeint library in scipy [107] package.

2. Cross-sections

The energy density transfer in Eq. (S20) displays the explicit cross-section dependence. Below we give expressions of various cross-sections that are relevant in this work. We cross-checked the cross-section calculation through *Mathematica* with *FeynCalc* [108], *FeynArts* [109] and *FeynRules* [110] pipeline.

The s -channel production of light fermions from the i -th neutrino through ϕ has a cross-section given by⁴

$$\sigma_{\nu_{l,i} \nu_{l,i} \rightarrow \chi\chi} = \frac{1}{16\pi s} \lambda_{\phi\chi}^2 \left(\lambda_{\phi N} \frac{m_{\nu,i}}{M_{N,i}} \right)^2 \frac{(s - 4m_\chi^2)(s - 4m_{\nu,i}^2)}{(s - m_\phi^2)^2 + m_\phi^2 \Gamma_\phi^2}. \quad (\text{S25})$$

Assuming that $\lambda_{\phi\chi}, \lambda_{\phi N}$ are of order 1, the cross-section is largely suppressed by the mass ratio of light and heavy neutrinos. The cross-section is enhanced when $s \approx m_\phi^2 \gg m_\chi^2$, allowing us to use the narrow width approximation:

$$\sigma_{\nu_{l,i} \nu_{l,i} \rightarrow \chi\chi} \xrightarrow{s \rightarrow m_\phi^2} \lambda_{\phi\chi}^2 \lambda_{\phi\nu_{l,i}}^2 \frac{1}{16\pi \Gamma_\phi^2} \approx \frac{\lambda_{\phi\nu_{l,i}}^2}{\lambda_{\phi\chi}^2} \frac{16\pi}{m_\phi^2}, \quad (\text{S26})$$

where $\lambda_{\phi\nu_{l,i}}$ is the coupling between the SM-like neutrinos and the mediator, and is given by

$$\lambda_{\phi\nu_{l,i}} \equiv \lambda_{\phi N} \frac{m_{\nu,i}}{M_{N,i}} \ll 1. \quad (\text{S27})$$

To get the final expression, we used the fact that ϕ dominantly decays to χ since $\lambda_{\phi\chi} \gg \lambda_{\phi\nu_{l,i}}$, and

$$\Gamma_\phi \approx \frac{m_\phi \lambda_{\phi\chi}^2}{16\pi}. \quad (\text{S28})$$

To get the cross-section in flavor basis $\nu_{\alpha_1} \nu_{\alpha_2} \rightarrow \chi\chi$, we simplify multiply $\sigma_{\nu_{l,i} \nu_{l,i} \rightarrow \chi\chi}$ by $|U_{\alpha_1 i}|^2 |U_{\alpha_2 i}|^2$ from the PMNS matrix and sum over the mass eigenstates $i = 1, 2, 3$. Note that this cross-section does not explicitly depend on neutrino masses, but on the ratio given in Eq (S27).

In addition, χ can be produced via $\nu\nu \rightarrow \phi\phi$ by t and u -channel exchange of heavy neutrinos N^c . The cross-section for $\nu_{l,i} \nu_{l,i} \rightarrow \phi\phi$ is equivalent to that of $\nu_{l,i} \nu_{l,i} \rightarrow \phi(\chi\chi)\phi(\chi\chi)$ since the branching ratio of $\phi \rightarrow \chi\chi$ is approximately 1. The cross-section is given by

$$\begin{aligned} \sigma_{\nu_{l,i} \nu_{l,i} \rightarrow \phi\phi} &= \frac{\lambda_{\phi\nu_{l,i}}^2 \lambda_{\phi N}^2}{128\pi s} \left[\frac{8f(s)}{1 + \frac{s}{M_{N,i}^2} g_i(s)^2} - 24f(s) + \frac{16 \left(6g_i(s)^2 + 4g_i(s) + 1 + \frac{4M_{N,i}^2}{s} \right)}{(1 + 2g_i(s))} \tanh^{-1} \left(\frac{f(s)}{1 + 2g_i(s)} \right) \right] \\ &\xrightarrow{M_N^2 \gg m_\phi^2, s} \frac{\lambda_{\phi\nu_{l,i}}^2 \lambda_{\phi N}^2}{8\pi M_{N,i}^2} \left(1 - \frac{s}{M_{N,i}^2} \right) f(s), \end{aligned} \quad (\text{S29})$$

where $f(s) \equiv \sqrt{1 - \frac{4m_\phi^2}{s}}$ and $g_i(s) \equiv \frac{M_{N,i}^2 - m_\phi^2}{s}$. Note that the expression takes a much simplified form in the limit of $M_N^2 \gg m_\phi^2, s$. This process needs to be suppressed compared to the neutrino interaction via W/Z bosons at early times in order to avoid populating χ sector prematurely (equivalent to avoiding $N_{\text{eff}}^{\text{tot}}$ bound). Our numerical scan comprises of parameter space where $\nu\nu \rightarrow \phi\phi$ is never important before BBN; see Fig. 1 top panel. This can always be achieved by choosing a large enough M_N .

The χ self-interaction cross-section is given by

$$\sigma_{\chi\chi \rightarrow \chi\chi} = \frac{\lambda_{\phi\chi}^4}{16\pi s^2 (m_\phi^2 - s)^2} \left[\frac{2 \left(5m_\phi^8 - 9m_\phi^6 s + 4m_\phi^2 s^3 \right) \log \left(\frac{m_\phi^2}{m_\phi^2 + s} \right)}{2m_\phi^2 + s} + \frac{s \left(5m_\phi^6 - 9m_\phi^4 s + 6s^3 \right)}{m_\phi^2 + s} \right], \quad (\text{S30})$$

⁴ We indicate $\nu_{l,i}$ as light neutrinos in mass eigenstates.

assuming $m_\chi^2 \ll s, m_\phi^2$. In the limit $m_\phi^2 \gg s$,

$$\sigma_{\chi\chi \rightarrow \chi\chi} \approx \frac{5\lambda_{\phi\chi}^4 s}{96\pi m_\phi^4} + \mathcal{O}\left(\frac{s^2}{m_\phi^6}\right), \quad (\text{S31})$$

which takes the form of $\frac{s}{12\pi} G_{\text{eff}}^2$, where G_{eff} characterizes the effective self-interaction among dark radiation. This has the same form as the cross-section of $\nu - \nu$ scattering in the SM assuming the interaction Lagrangian $G_F \bar{\nu}\nu\bar{\nu}\nu$.

Lastly, the heavy sterile neutrinos can be thermalized with the SM bath through mixing with the active neutrinos via processes like $e\nu_l \rightarrow e\nu_h$, or pair production, via exchange of W/Z or ϕ in $\nu_l\nu_l \rightarrow \nu_h\nu_h$. The process $e\nu_l \rightarrow e\nu_h$ has the same form of cross-section as the SM process $e\nu_l \rightarrow e\nu_l$, but scaled down by m_{ν_l}/M_N with a minimum energy requirement factor $\sqrt{1 - M_N^2/s}$. On the other hand, for the ν_h pair production, the Z mediated channel is suppressed at low energy, whereas the ϕ -mediated channel is more important. Below we give the differential cross-section of ϕ -exchanged pair production:

$$\begin{aligned} \frac{d\sigma_{\nu_{l,i}\nu_{l,i} \rightarrow \nu_h\nu_h}}{d\Omega} \approx & \frac{1}{16\pi^2 s} \sqrt{\frac{s - 4M_N^2}{s}} \lambda_{\phi N}^4 \frac{m_{\nu_{l,i}}^2}{M_N^2} \left[3 + M_N^4 \left(\frac{1}{t^2} - \frac{1}{tu} + \frac{1}{u^2} \right) \right. \\ & - M_N^2 \left(\frac{u}{st} + \frac{t}{su} + \frac{2s}{tu} + \frac{2}{s} - \frac{1}{t} - \frac{1}{u} \right) \\ & \left. + \frac{1}{2} \left(\frac{s^2}{tu} + \frac{t^2}{su} + \frac{u^2}{st} - \frac{t}{s} - \frac{s}{t} - \frac{u}{s} - \frac{s}{u} - \frac{u}{t} - \frac{t}{u} \right) \right]. \quad (\text{S32}) \end{aligned}$$

3. Interaction Rates

To estimate whether a process comes into equilibrium with the thermal bath, the minimum requirement is to have them in contact with the bath particles. When this happens can be estimated using the ratio of the thermally averaged interaction rate to the Hubble rate, Γ/H .

Consider a $2 \rightarrow 2$ process $p_1 + p_2 \rightarrow p_3 + p_4$, where the two initial-state particles are of identical mass m . Suppose that the initial-state particles are part of the early universe bath. To estimate when this process begins to become efficient, we compare the Hubble rate with the rate of this process [111], which is defined as $\Gamma \equiv n\langle\sigma v\rangle$, where n is the density of the initial state particles and $\langle\sigma v\rangle$ is the thermally averaged cross-section defined as:

$$\langle\sigma v\rangle = \frac{\int d^3p_1 \int d^3p_2 \sigma v e^{-E_1/T - E_2/T}}{\int d^3p_1 \int d^3p_2 e^{-E_1/T - E_2/T}}, \quad (\text{S33})$$

where the denominator is simply given by $(4\pi m^2 T K_2(\frac{m}{T}))^2$. To obtain an expression for the numerator, we express the relative velocity as $v = \frac{1}{2E_1 E_2} \sqrt{s(s - 4m^2)}$. Defining $E_\pm = E_1 \pm E_2$, the numerator can be simplified as

$$\begin{aligned} \int d^3p_1 \int d^3p_2 \sigma v e^{-(E_1 + E_2)/T} &= \pi^2 \int_{4m^2}^{\infty} ds \sigma \sqrt{s(s - 4m^2)} \int_{\sqrt{s}}^{\infty} dE_+ e^{-E_+/T} \int dE_- \\ &= 2\pi^2 \int_{4m^2}^{\infty} ds \sigma(s - 4m^2) \int dE_+ e^{-E_+/T} \sqrt{E_+^2 - s} \\ &= 2\pi^2 T \int_{4m^2}^{\infty} ds \sigma(s - 4m^2) \sqrt{s} K_1\left(\frac{\sqrt{s}}{T}\right). \quad (\text{S34}) \end{aligned}$$

where we used $|E_-| \leq \sqrt{1 - \frac{4m^2}{s}} \sqrt{E_+^2 - s}$. In summary, we obtain

$$\Gamma_{12 \rightarrow 34} = \frac{g_1}{16\pi^2 m^2 K_2(\frac{m}{T})} \int_{4m^2}^{\infty} ds \sigma_{12 \rightarrow 34}(s - 4m^2) \sqrt{s} K_1\left(\frac{\sqrt{s}}{T}\right) \xrightarrow{\frac{m}{T} \rightarrow 0} \frac{g_1}{32\pi^2 T^2} \int_{4m^2}^{\infty} ds \sigma_{12 \rightarrow 34} s^{3/2} K_1\left(\frac{\sqrt{s}}{T}\right). \quad (\text{S35})$$

Here, we present the explicit expressions for Γ/H using cross-sections from the previous subsection. Below are the

results assuming $m_\chi, m_\nu \ll \sqrt{s}$,

$$\Gamma_{\nu\nu\rightarrow\chi\chi} \approx \frac{\lambda_{\phi\chi}^2 \left(\frac{\lambda_{\phi N} m_\nu}{M_N}\right)^2}{256\pi^3 T^2} \int_{(m_\phi - \Gamma_\phi)^2}^{(m_\phi + \Gamma_\phi)^2} ds \frac{s^{1/2} K_1\left(\frac{\sqrt{s}}{T}\right) s^2}{(s - m_\phi^2)^2 + m_\phi^2 \Gamma_\phi^2} \approx \left(\frac{\lambda_{\phi N} m_\nu}{M_N}\right)^2 K_1\left(\frac{m_\phi}{T}\right) \frac{m_\phi^3}{4\pi^2 T^2}, \quad (\text{S36})$$

$$\Gamma_{\chi\chi\rightarrow\chi\chi} \approx \frac{5\lambda_{\phi\chi}^4}{16\pi^3 T^2 96m_\phi^4} \int_{4m_\chi^2}^{\infty} ds s^{5/2} K_1\left(\frac{\sqrt{s}}{T}\right) \approx \lambda_{\phi\chi}^4 \frac{5T^5}{2\pi^3 m_\phi^4} \text{ when } m_\chi \ll \sqrt{s} \ll m_\phi, \quad (\text{S37})$$

$$\Gamma_{\nu\nu\rightarrow\phi\phi} \approx \frac{\lambda_{\phi\chi}^2 m_\nu^2 \lambda_{\phi N}^4}{256\pi^3 T^2 M_N^6} \int_{4m_\phi^2}^{\infty} ds s^{5/2} K_1\left(\frac{\sqrt{s}}{T}\right) \approx \lambda_{\phi\chi}^2 \left(\frac{m_\nu}{M_N}\right)^2 \lambda_{\phi N}^4 \frac{3T^5}{\pi^3 M_N^4} \text{ when } m_\phi \ll \sqrt{s} \ll M_N, \quad (\text{S38})$$

$$\Gamma_{\phi\rightarrow\chi\chi} \approx \Gamma_\phi \frac{K_1(m_\phi/T)}{K_2(m_\phi/T)} \quad \text{where } \Gamma_\phi \text{ is decay width of } \phi \text{ in rest frame.} \quad (\text{S39})$$

Assuming $T > m_\phi$, the ratio of the interaction rate of ϕ to Hubble rate reduces to

$$\frac{\Gamma_{\phi\rightarrow\chi\chi}}{H} \sim \lambda_{\phi\chi}^2 m_\phi \left(\frac{m_\phi}{T}\right) \frac{M_{\text{pl}}}{T^2}. \quad (\text{S40})$$

This ratio is much bigger than 1 for all the model parameters and temperatures of interest in this work, which means that ϕ is never long-lived enough to be part of the bath. This is why we do not track the evolution of ϕ in the main text.

4. Calculation of N_{eff}^ν

In Fig. 2, we show the resultant N_{eff}^ν for $n_\chi = 1$ (left panel) and $n_\chi = 2$ (right panel) after $\nu - \chi$ decoupling from solving the Boltzmann equations (S21–S24). Here we give more details of this analysis.

In Fig. S2 we show the temperature evolution for χ and ν at a fixed neutrino mass $\sum m_\nu = 0.065$ eV and the number of DR flavor $n_\chi = 1$, but with different ϕ masses. This corresponds to $G_{\text{eff}} \in (10^{-5} \text{ MeV}^{-2}, 10^{-1} \text{ MeV}^{-2})$. It can be seen that m_ϕ only affects when neutrinos start to be cooled, since the cooling occurs resonantly through $\nu\nu \rightarrow \phi \rightarrow \chi\chi$ when $T_\nu \sim m_\phi$. It does not affect the final N_{eff}^ν as long as the $\nu - \chi$ thermalization is efficient.

In Fig. S3 we show the temperature evolution for χ and ν at a fixed $m_\phi = 1$ MeV for difference choices of $\sum m_\nu$. This corresponds to $G_{\text{eff}} \approx 10^{-5} \text{ MeV}^{-2}$ in Fig. 2. Since the neutrino–mediator coupling in Eq.(S27) is proportional to the light to heavy neutrino mass ratio, $\sum m_\nu$ directly controls the overall size of $\sigma(\nu\nu \rightarrow \chi\chi)$, and hence, the $\nu \rightarrow \chi$ energy transfer efficiency. For $\sum m_\nu < 0.03$ eV, cooling is insufficient as indicated in the lower right corner of Fig. 2. This is reflected in the negligible difference between N_{eff}^ν and $N_{\text{eff}}^{\text{tot}}$ in the first row of Fig. S3. For $\sum m_\nu > 0.65$ eV, $\sigma(\nu\nu \rightarrow \chi\chi)$ is large enough that the cooling takes off immediately when the temperature is close to the ϕ mass (MeV). Under this condition, the neutrino is still in thermal contact with e^\pm , implying that they are indirectly coupled with γ as well. The production of χ lowers the neutrino temperature and this leads to energy flow of $e \rightarrow \nu$ to accommodate thermal equilibrium. Due to the strong coupling between $e - \gamma$ before/during BBN, photon gets cooled accordingly. As a result, the system after BBN includes small portion of extra radiation, χ , which means that the total N_{eff} is higher than $N_{\text{eff}}^{\text{SM}}$.

In Fig. S4, we show $n_\chi = 1, 2$ results as we increase $m_N/\lambda_{\phi N}$ to be 10 times larger than that of Fig. 2. This results in a 100 times smaller $\sigma(\nu\nu \rightarrow \phi \rightarrow \chi\chi)$, thus a reduced efficiency in $\nu - \chi$ energy transfer. This is reflected in the overall reduction in the light yellow region where neutrino cooling is maximal.

5. Normal Ordering Benchmarks

In the analyses above it is assumed that the neutrinos have degenerate masses. In Fig. S5 we show benchmarks with normal ordering with the lightest neutrino mass $m_\nu^{\text{min}} = 1$ meV. Compared to Fig. S2, the overall cooling of neutrinos is not affected for $m_\phi \lesssim 100$ keV. However, in this case, different neutrino species may not be in equilibrium after cooling, which is reflected in different evolution trajectories undergone by T_{ν_μ} and T_{ν_e} . The reason is that ν_e comprises the first two lightest mass eigenstates mostly, thus contributing less to $\nu - \chi$ thermalization, since the neutrino–mediator coupling is directly proportional to neutrino masses. This is especially prominent when m_ϕ becomes larger, where ν_e does not contribute at all to $\nu - \chi$ thermalization and thus has the same temperature as that of the standard cosmology case.

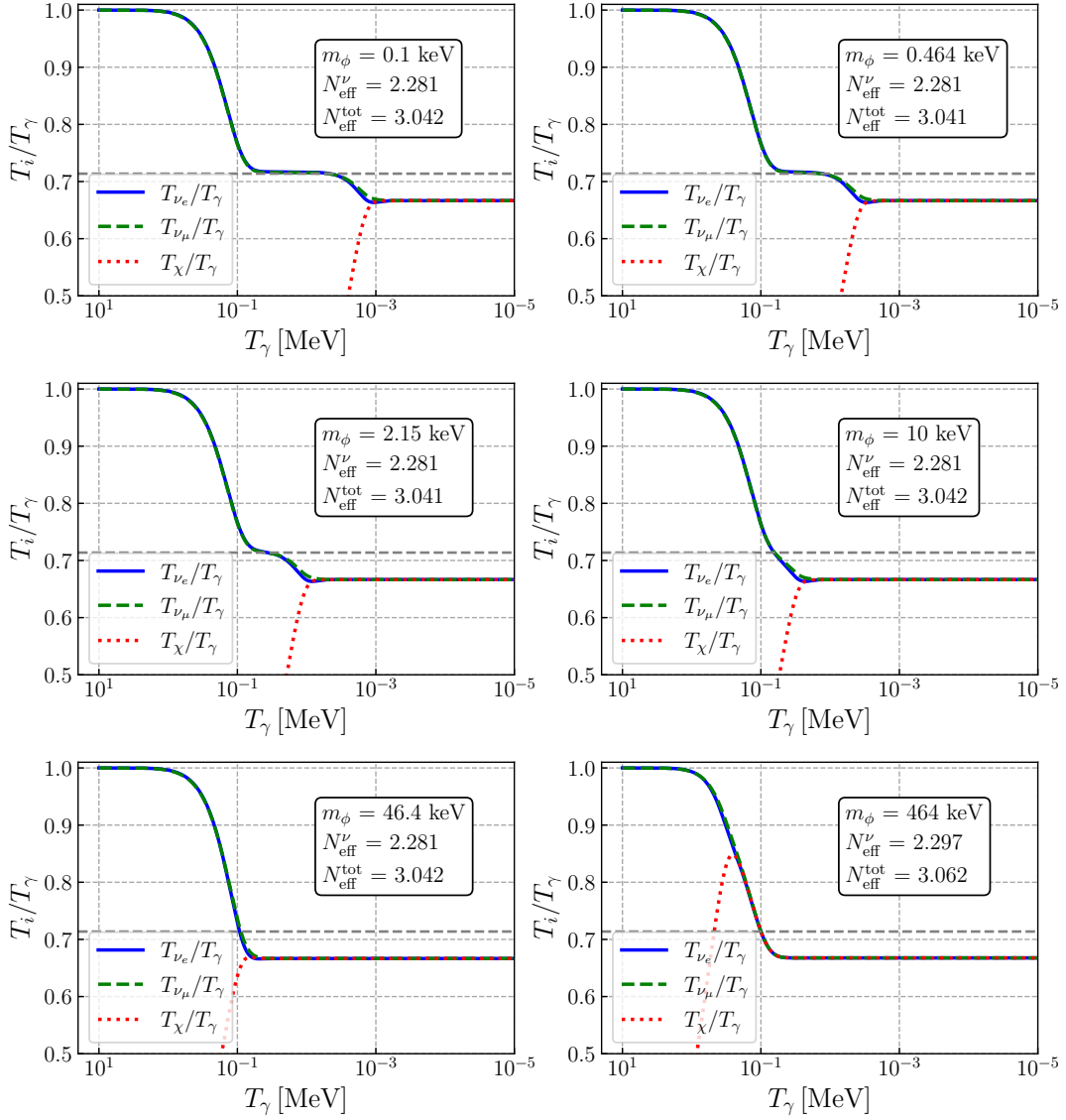


FIG. S2: Temperature evolution of ν and χ when varying only m_ϕ . Here $\sum m_\nu = 0.065$ eV and $n_\chi = 1$. Other parameters are as in Fig. 2. Cooling is efficient for all values of m_ϕ but with different initialization times.

6. Increasing DR Flavors

The previous subsections focused on scenarios with $n_\chi = 1$ or 2, mimicking a flavor specific self-interacting neutrino cosmology where only fractions of neutrinos are free-streaming after decoupling. In this subsection, we take the liberty to choose as many DR flavors as we wish. In Fig. S6 we show the neutrino coupling for a scenario with $n_\chi = 40$ in the MI (left panel) and SI (right panel) modes. It is clear that the thermalization is efficient for both modes, so that the neutrino contribution to N_{eff} is suppressed: $N_{\text{eff}}^\nu = 3(1 + n_\chi/3)^{-1} \approx 0.2$ in this case. The large n_χ enables an almost complete depletion of neutrino energy, hence free-streaming neutrinos are almost entirely replaced by self-interacting DR, mimicking a flavor-universal self-interacting neutrino in cosmology, while evading the cosmological constraint on $\sum m_\nu$, as well as the laboratory constraints on neutrino self-interaction (see Section B above).

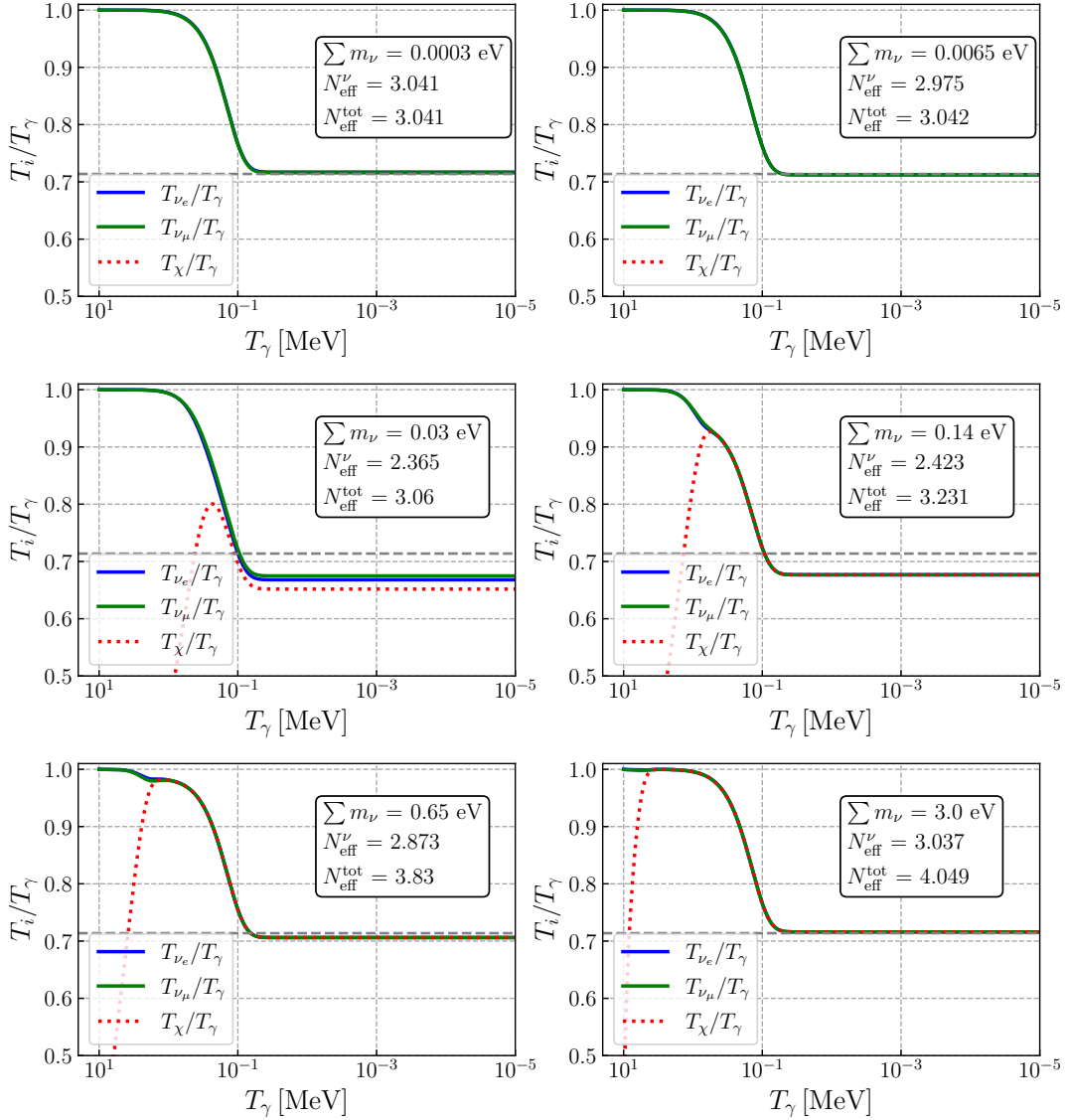


FIG. S3: Temperature evolution of ν and χ when varying only $\sum m_\nu$. Here $m_\phi = 1$ MeV, $n_\chi = 1$, and other parameters are as in Fig. 2. As $\sum m_\nu$ increases, the coupling of $\nu - \phi$ increases (Eq. 5), hence increasing the $\nu \rightarrow \chi$ energy transfer efficiency. This results in an insufficient cooling for too small $\sum m_\nu$ in the first row. For large enough $\sum m_\nu$, the cooling immediately takes off at a temperature close to ϕ mass. This results in a significant increase in $N_{\text{eff}}^{\text{tot}}$ in the last row, which would be severely constrained by BBN.

D. Cosmological Analysis

In this section, we provide more details for our cosmological analysis. Massive free-streaming neutrinos follow the standard Boltzmann hierarchy as given in Ref. [112]. The Boltzmann moments of the perturbation to the DR distribution function is defined as follows [112]:

$$f_\chi(\mathbf{q}, \mathbf{k}, \tau) = \bar{f}_\chi(q, \tau)(1 + \Psi(\mathbf{q}, \mathbf{k}, \tau)), \quad (\text{S41})$$

where $\bar{f}_\chi(q, \tau)$ is the background Fermi-Dirac distribution function for DR, Ψ is the perturbation on it, τ is the conformal time, \mathbf{k} is the wave vector of Fourier mode, $\mathbf{q} = a\mathbf{p}$ is the comoving momentum, with a being the scale

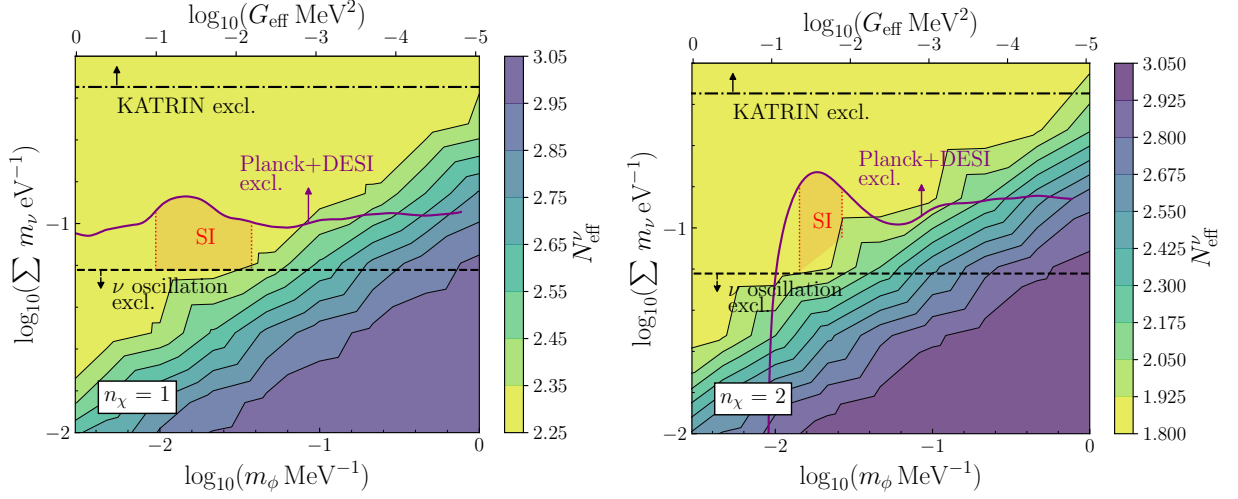


FIG. S4: $(\sum m_\nu, m_\phi)$ parameter scan result with $n_\chi = 1$ (Left) and $n_\chi = 2$ (Right) with $m_N/\lambda_{\phi N} = 1000$ MeV, $\lambda_{\phi\chi} = 0.003$, assuming degenerate neutrino masses.

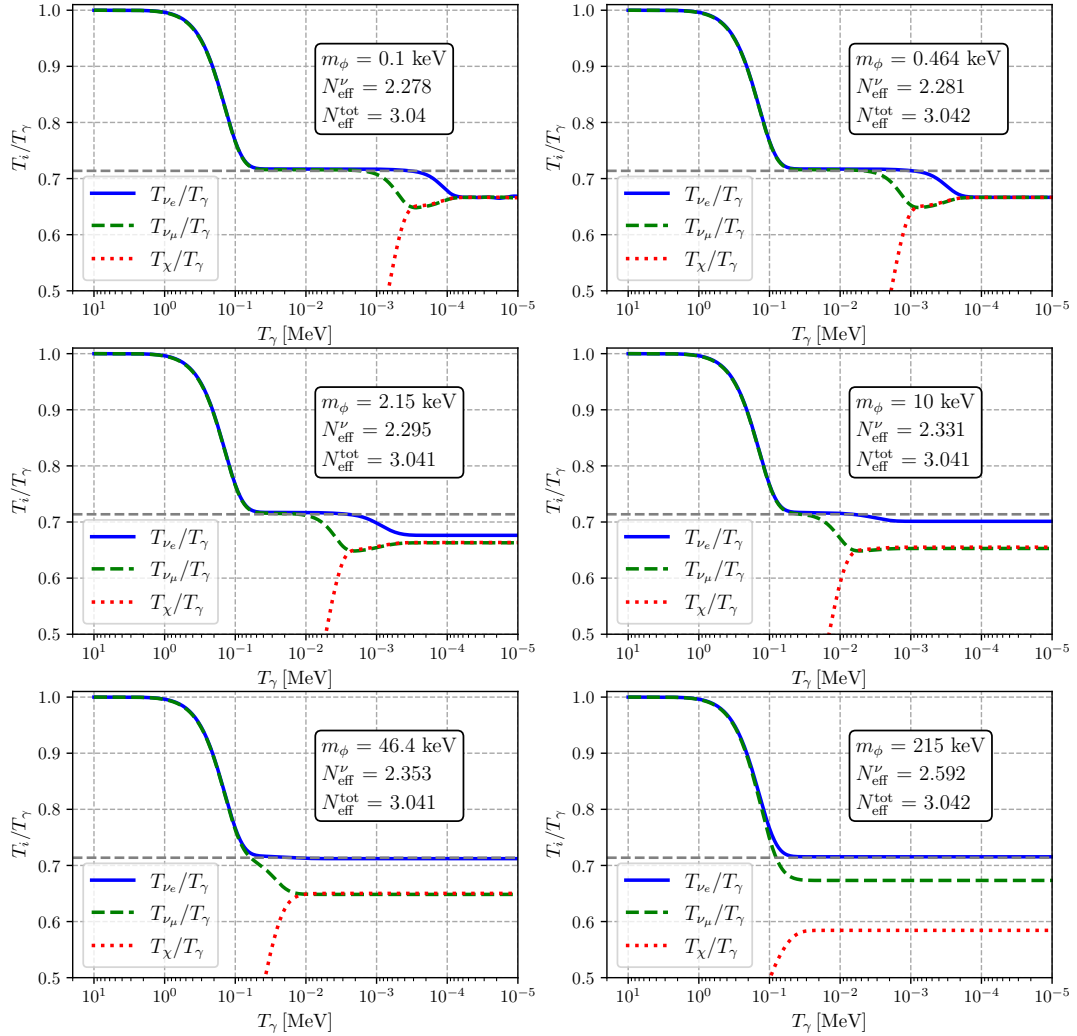


FIG. S5: Temperature evolution of ν and χ when varying only m_ϕ . Normal ordering is assumed with the lightest neutrino mass $m_\nu^{\min} = 1$ meV and with $n_\chi = 1$, while the other parameters are the same as in Fig. 2.

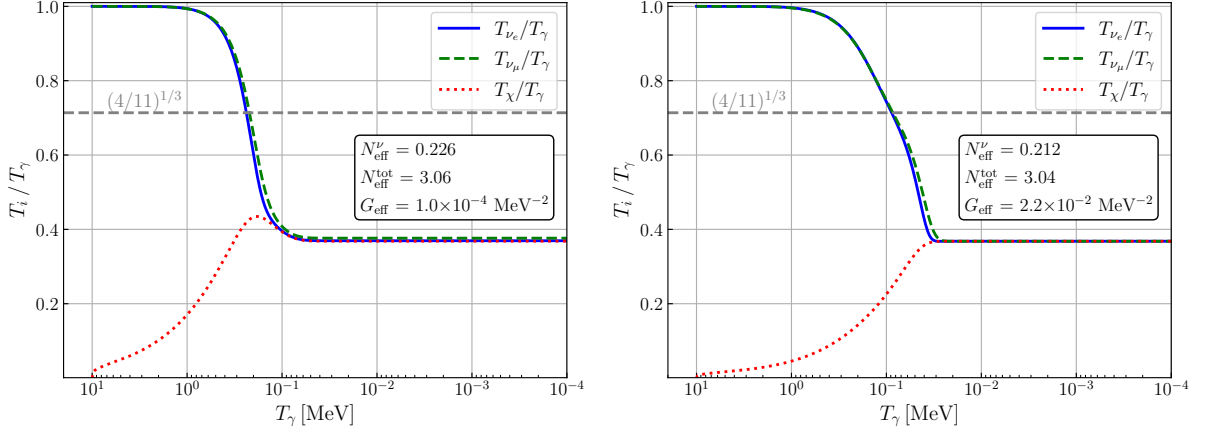


FIG. S6: Temperature evolution of ν and χ for $n_\chi = 40$. Here we have taken $m_N/\lambda_{\phi N} = 100$ MeV and $\sum m_\nu = 0.09$ eV assuming degenerate neutrino masses. The left (right) panel is for the MI (SI) mode with $G_{\text{eff}} = 1.0 \times 10^{-4}$ MeV^{-2} (2.2×10^{-2} MeV^{-2}). Note the sharp drop in the neutrino temperature.

factor and \mathbf{p} the proper momentum. The momentum-averaged perturbation is given by

$$F_\chi(\hat{\mathbf{q}}, \mathbf{k}, \tau) \equiv \frac{\int dq q^3 \bar{f}_\chi \Psi}{\int dq q^3 \bar{f}_\chi} \equiv \sum_{\ell=0}^{\infty} (-i)^\ell (2\ell+1) F_{\chi\ell}(k, \tau) P_\ell(\hat{\mathbf{q}} \cdot \hat{\mathbf{k}}), \quad (\text{S42})$$

where P_ℓ are the Legendre polynomials, and $F_{\chi\ell}$ are the momentum-averaged ℓ -th multipoles of the perturbation.

The Boltzmann hierarchy for moments are given by

$$\dot{\delta}_\chi = -\frac{4}{3}\theta_\chi - \frac{2}{3}\dot{h}, \quad (\text{S43})$$

$$\dot{\theta}_\chi = k^2 \left(\frac{1}{4}\delta_\chi - \sigma_\chi \right), \quad (\text{S44})$$

$$\dot{F}_{\chi 2} = \frac{8}{15}\theta_\chi - \frac{3}{5}kF_{\chi 3} + \frac{4}{15}\dot{h} + \frac{8}{5}\dot{\eta} - aG_{\text{eff}}^2 T_\chi^5 \alpha_2 F_{\chi 2}, \quad (\text{S45})$$

$$\dot{F}_{\chi\ell} = \frac{k}{2\ell+1} (\ell F_{\chi(\ell-1)} - (\ell+1)F_{\chi(\ell+1)}) - aG_{\text{eff}}^2 T_\chi^5 \alpha_\ell F_{\chi\ell}, \quad \ell \geq 3. \quad (\text{S46})$$

Here, dot represents derivative w.r.t. the conformal time τ ; h and η are the metric perturbations in the synchronous gauge; $\delta_\chi = F_{\chi 0}$ is the density fluctuation, $\theta_\chi = (3/4)kF_{\chi 1}$ is the divergence of fluid velocity, $\sigma_\chi = F_{\chi 2}/2$ is the shear stress; G_{eff} is defined as in Eq. (6). In this analysis, we set $\alpha_\ell \approx \alpha_2 = 0.424$ [113]. Note that, although different α_ℓ values differ slightly from α_2 , the differences have a negligible impact on the solution of the Boltzmann hierarchy. We implemented these modifications in the Boltzmann solver Cosmic Linear Anisotropy Solving System (CLASS), which we used for our Markov Chain Monte Carlo analysis [114, 115].

Since we expect the posterior to be bi-modal, we used Nested sampling for our primary analysis with the Planck and DESI data using **Multinest** [116–119] and **Montepython** [120, 121]. We used the priors on the baryon density $\omega_b \equiv \Omega_b h^2$, cold dark matter density $\omega_c \equiv \Omega_c h^2$, Hubble constant today $H_0 \equiv 100h$ km/s/Mpc, the initial super-horizon amplitude of the curvature perturbations A_s at $k = 0.05$ Mpc^{-1} , the primordial spectral index n_s , reionization optical depth τ_{reio} , the effective self-interaction strength G_{eff} , and the sum of neutrino masses $\sum m_\nu$ as given in Table S1 for the primary runs.

Since Multinest is very inefficient with a large number of parameters, we used the nuisance marginalized Planck likelihood (**Plik_lite**). The ‘Planck’ dataset is comprised of low- ℓ TT ($\ell < 30$), low- ℓ EE ($\ell < 30$), high- ℓ TTTEEE **plik_lite** ($\ell \geq 30$) and lensing likelihood [87, 88]. We also use the BAO scale measurements from Dark Energy Spectroscopic Instrument (DESI) Data Release 1 (DR1) [89, 122]. In our analysis, we have set the total $N_{\text{eff}} = 3.044$ [90] since we focus on resonant conversion of neutrinos to DR *after* BBN. We set $N_{\text{eff}}^\chi = 0.75(1.2)$ and $N_{\text{eff}}^\nu = 2.294(1.244)$ for $n_\chi = 1(2)$. For notational brevity we use $N_{\text{eff}}^\nu = 2.25(1.2)$ in the text. We also choose the neutrino flavors to have degenerate mass for the cosmological analysis.

The triangle plot for the posteriors from the analysis with Planck and Planck + DESI is shown in Fig. S7. The SI mode significance is increased by the addition of the DESI BAO dataset. The likely reason is that the SI mode value

Parameters	Prior
$10^2\omega_b$	[1.0, 4.0]
ω_c	[0.08, 0.16]
H_0 [km/s/Mpc]	[55.0, 85.0]
$\log(10^{10}A_s)$	[2.0, 4.0]
n_s	[0.8, 1.1]
τ_{reio}	[0.004, 0.25]
$\log_{10}(G_{\text{eff}}\text{MeV}^2)$	[-5.0, 1.0]
$\sum m_\nu$	[0, 1.5]

TABLE S1: Flat prior ranges for the Nested sampling analysis.

Mode	$\log_{10}(G_{\text{eff}}\text{MeV}^2)$ Prior
MI	[-5.0, -2.5]
SI	[-2.5, 0.0]

TABLE S2: Priors on $\log_{10}(G_{\text{eff}}\text{MeV}^2)$ parameter for the separate MI and SI mode analyses.

Parameters	Planck			
	$0.75N_\chi + 2.25N_\nu$		$1.2N_\chi + 1.8N_\nu$	
	MI	SI	MI	SI
$10^2\omega_b$	2.23 ± 0.02	2.24 ± 0.02	2.23 ± 0.02	2.24 ± 0.02
ω_c	0.120 ± 0.001	0.120 ± 0.001	0.120 ± 0.001	0.121 ± 0.001
H_0 [km/s/Mpc]	$67.1^{+1.1}_{-0.6}$	$67.5^{+1.1}_{-0.7}$	$67.0^{+1.1}_{-0.6}$	$67.6^{+1.1}_{-0.6}$
$\log(10^{10}A_s)$	3.05 ± 0.02	3.03 ± 0.02	3.05 ± 0.02	3.02 ± 0.02
n_s	$0.963^{+0.005}_{-0.004}$	$0.957^{+0.005}_{-0.005}$	$0.962^{+0.005}_{-0.005}$	0.953 ± 0.005
τ_{reio}	0.055 ± 0.008	$0.055^{+0.007}_{-0.008}$	0.055 ± 0.008	$0.055^{+0.007}_{-0.008}$
σ_8	$0.809^{+0.02}_{-0.007}$	$0.809^{+0.02}_{-0.008}$	$0.809^{+0.02}_{-0.007}$	$0.810^{+0.02}_{-0.008}$
$\log_{10}(G_{\text{eff}}\text{MeV}^2)$	< -3.34	< -1.23	< -3.48	$-1.7^{+0.3}_{-0.2}$
$\sum m_\nu$ [eV]	< 0.126	< 0.121	< 0.159	< 0.157
Ω_m	$0.319^{+0.008}_{-0.02}$	$0.316^{+0.008}_{-0.01}$	$0.320^{+0.008}_{-0.02}$	$0.315^{+0.008}_{-0.02}$

TABLE S3: 1σ parameter constraints for the separate MI and SI mode analyses with Planck dataset.

Parameters	Planck + DESI			
	$0.75N_\chi + 2.25N_\nu$		$1.2N_\chi + 1.8N_\nu$	
	MI	SI	MI	SI
$10^2\omega_b$	2.25 ± 0.01	2.25 ± 0.01	2.25 ± 0.01	2.25 ± 0.01
ω_c	0.1185 ± 0.0009	0.1191 ± 0.0009	0.1185 ± 0.0009	0.119 ± 0.001
H_0 [km/s/Mpc]	$68.4^{+0.5}_{-0.4}$	68.6 ± 0.5	68.4 ± 0.4	68.6 ± 0.5
$\log(10^{10}A_s)$	3.05 ± 0.02	3.03 ± 0.02	3.05 ± 0.02	3.03 ± 0.02
n_s	0.967 ± 0.004	$0.959^{+0.006}_{-0.004}$	$0.967^{+0.005}_{-0.004}$	$0.957^{+0.005}_{-0.004}$
τ_{reio}	0.058 ± 0.008	0.057 ± 0.007	$0.058^{+0.007}_{-0.008}$	$0.057^{+0.007}_{-0.008}$
σ_8	$0.817^{+0.008}_{-0.007}$	$0.815^{+0.01}_{-0.008}$	$0.818^{+0.008}_{-0.007}$	$0.819^{+0.01}_{-0.007}$
$\log_{10}(G_{\text{eff}}\text{MeV}^2)$	< -3.28	$-1.3^{+0.3}_{-0.9}$	< -3.44	$-1.7^{+0.3}_{-0.2}$
$\sum m_\nu$ [eV]	< 0.0471	< 0.0518	< 0.0575	< 0.0667
Ω_m	0.302 ± 0.006	$0.302^{+0.005}_{-0.006}$	$0.302^{+0.005}_{-0.006}$	0.302 ± 0.006

TABLE S4: 1σ parameter constraints for the separate MI and SI mode analyses with Planck dataset.

of the total matter density Ω_m is slightly smaller than the MI mode and the DESI likelihood prefers a smaller value of Ω_m . The qualitative features of our analysis are expected to remain unchanged while considering DESI 3-year

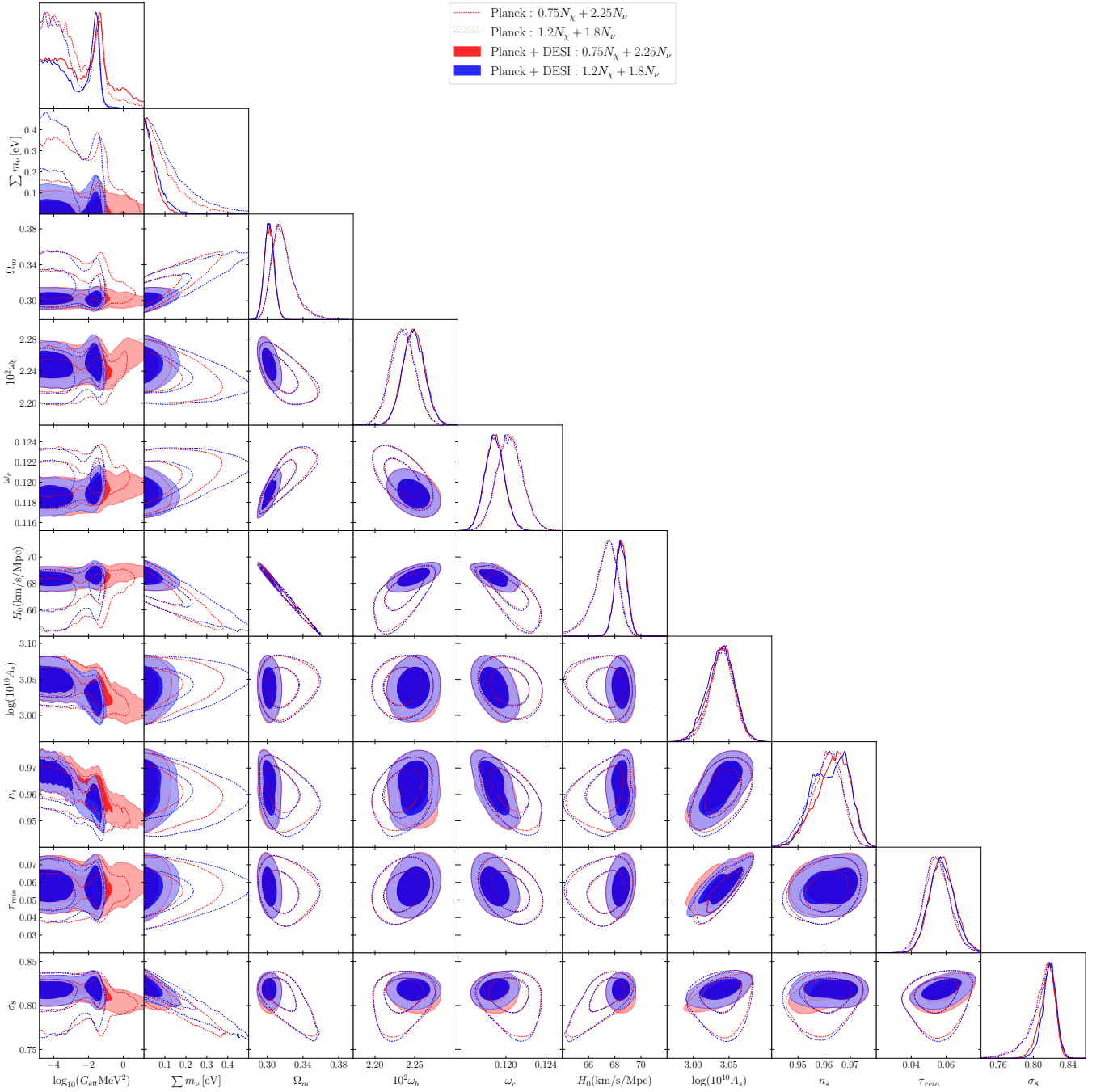


FIG. S7: Triangle plot of all the relevant parameters for our cosmological analysis with Planck and Planck + DESI datasets.

(DESI-II) data release [7, 123], since DESI-I and DESI-II are largely consistent with each other.

To study the individual modes, we also performed a separate analysis where we choose different priors on $\log_{10}(G_{\text{eff}}/\text{MeV}^2)$ values to study MI and SI mode separately as shown in Table S2. Having separate priors guarantees that the distributions in the MI and SI modes are unimodal. Therefore, we used the Metropolis–Hastings algorithm [124, 125] for this analysis. We also used the full high- ℓ TTTEEE `plik` ($\ell \geq 30$) with all the nuisance parameters instead of the `plik_lite` likelihood used in the previous nested sampling analysis. For the rest of the parameters, we kept the prior ranges the same as those in Table S1. We show the parameter values for the mode-specific analysis in Table S3 and Table S4.